

## General Comments

Based on the Community Land Model version 4.5 (CLM4.5) framework, a new perennial crop sub-model (CLM-Palm) was developed in this study. The model structure was reasonable, and the parameters were comprehensively considered. In addition, the authors also analyzed the results logically. This research is novel and important to land surface model, particularly crop model, development and biodiversity studies. This manuscript can be accepted after clarifying several minor concerns.

## Answers to specific comments (line numbers refer to marked-up manuscript):

### Comments

**1.** To address the importance of oil palm, I suggest that the authors discuss the global total area of oil palm or the ratio of the Indonesia oil palm area to the global total oil palm area in the first paragraph.

**Answer 1:** We follow the suggestion to include this information in the first paragraph: “In 2013 the harvested area of oil palm plantations in Indonesia alone was 7.1 million ha, accounting for 42% of world total (17 million ha), followed by Malaysia’s 4.5 million ha (FAO, 2013). Indonesia’s consistently high growth rate of oil palm area (nearly 10% annually; Gunarso et al. 2013) in the last two decades has placed it as the largest global palm-oil producer, and yet it has planned to double its oil palm planted area from 9.7 million ha in 2009 to 18 million ha by 2020 (Koh and Ghazoul, 2010).” (Lines 50-55)

Here note the difference between oil palm harvested area and planted area from the references. FAOSTAT only provides data for harvested area, while the planted area including young oil palm plantations is larger.

**2.** Line 85, if “annual” is used as “occurring once every year”, it is an adjective. I suggest using “annual growing season” here.

**Answer 2:** Here “annuals” were referring to “annual crops” and now we use the suggested phrase. We also distinguish between “perennial deciduous crops” and “perennial evergreen crops”. Georgescu et al. (2011) didn’t really simulate the perennial crops in the way that they should grow for multiple years. They extended the 6-month growing season of annual crops to 8 months so as to represent the longer growing season of perennial energy crops but their simulations were only run for one year. This is still very different from the perennial evergreen crop simulated by CLM-Palm. We revise the sentence to clarify the difference: “Attempts were also made to evaluate the climate effects of perennial deciduous crops, e.g. by extending the annual growing season to simulate earlier green-up and lagged senescence (Georgescu et al., 2011). However, the perennial evergreen crops such as oil palm, cacao, coffee, rubber, coconut, etc. and their long-term biophysical processes are not represented

in the above land models yet, despite the worldwide growing demand (FAO, 2013).” (Lines 89-94)

3. Line 102, change “In this context” to “In this study” or “In this paper”.

**Answer 3:** Changed to “In this study” (Line 108).

4. In the supplement file, GDD and PLAI were not defined before use.

**Answer 4:** Now they are defined in the supplementary materials too.

5. The authors can define C, as “carbon (C)”, when it first appears; then, use C in the rest of the manuscript. Or use carbon everywhere. Using C and carbon randomly is not a standard way for scientific writing. Nitrogen/N has the same issue.

**Answer 5:** We now define and use the terms C and N consistently in the manuscript.

6. I suggest inserting a table in Section 3.1 to indicate the general information, such as climate condition, fertilization period, of the eight sites. A table like this can make Section 3.1 more straightforward, and the readers can check each site more quickly, which is helpful for understanding Section 4.1.

**Answer 6:** We follow the suggestion to add Table 1 as below and it is referred to in the text of section 3.1 (Lines 293, 313; Table in page 25).

Table 1. Site conditions and N fertilization records at the calibration and validation plots.

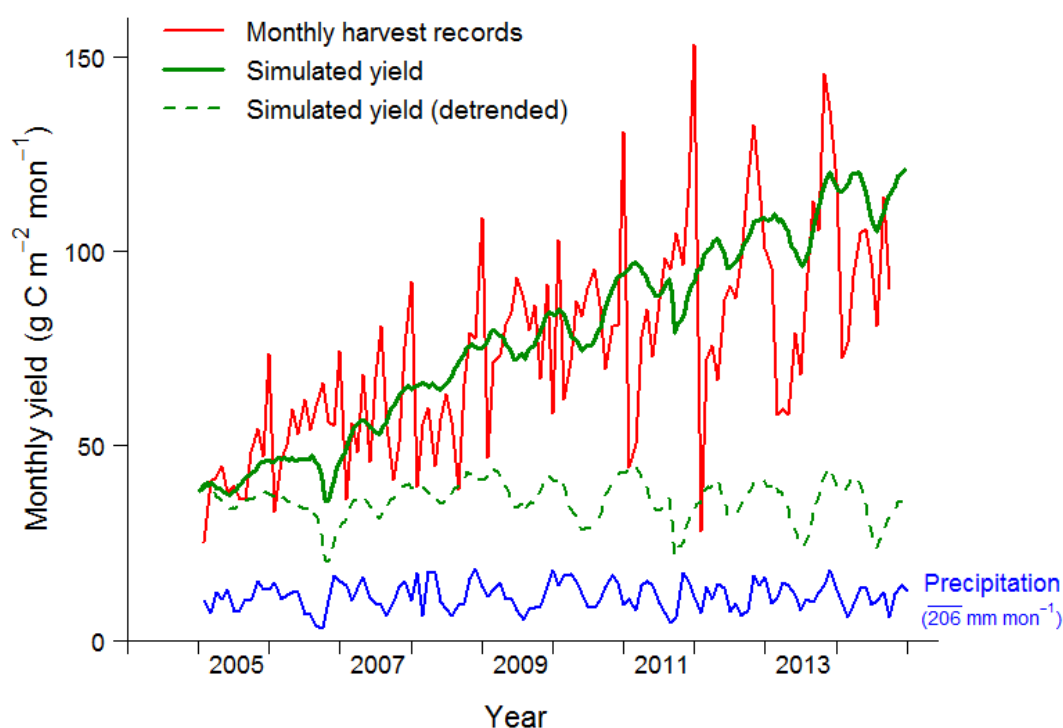
Site	Year of planting	Precipitation (mm yr <sup>-1</sup> )	Soil type	Fertilization		Comments
				amount (kg N ha <sup>-1</sup> yr <sup>-1</sup> )	period	
PTPN-VI	2002	2567	loam Acrisol	456	2008-2014	industrial plantation; others are smallholders
Pompa Air	2012	2567	loam Acrisol	-	-	N fertilization from 6-year old onward
HO1	1997	2567	loam Acrisol	96	2003-2014	regular fertilization
HO2	1999	2567	loam Acrisol	96	2005-2014	regular fertilization
HO3	1996	2567	loam Acrisol	96	2002-2014	regular fertilization

HO4	2003	2567	loam Acrisol	96	2009-2014	regular fertilization
BO2	2000	2902	clay Acrisol	24	2006-2012	reduced fertilization
BO3	2001	2902	clay Acrisol	24	2007-2012	reduced fertilization
BO4	2002	2902	clay Acrisol	24	2008-2012	reduced fertilization
BO5	2004	2902	clay Acrisol	24	2010-2012	reduced fertilization

7. Line 431, the described fluctuation between yield and precipitation is not very obvious. Can the authors give more detailed description or show the detrended curves?

**Answer 7:** We add the detrended curve of simulated yield in Fig. 7 and also more explanation on the correlation analysis. See below new figure and revised sentence: “The simulated monthly yield has less seasonal fluctuation, but it corresponds to the general pattern of precipitation (Fig. 7). A significant positive linear correlation exists between simulated yield (detrended to minimize phenological effects) and the accumulative precipitation of a 120-day period (the main fruit-filling and oil synthesis period) before each harvest event (Pearson's  $r=0.32$ ,  $p$ -value  $< 1E-06$ ).” (Lines 439-444)

Also see the answer to comment 9.



8. Line 483, in my view, NPP is (GPP – maintenance respiration – growth respiration) for the entire plant. So, I cannot understand what “leaf NPP” is. In addition, I wonder why leaf litter production is the only measurement included into field measured NPP? Can the authors re-phase this sentence or explain this sentence more?

**Answer 8:** It is fairly common among ecophysiologicalists to split NPP per organ, i.e. leaves, roots, stem and fruits. There are a lot of examples in the literature, e.g. Navarro et al. (2008) and Kotowska et al. (2015a) cited in this study or Campioli et al. (2011) (Biogeosciences, 8, 2481–2492, doi:10.5194/bg-8-2481-2011).

We considered leaf litter production as well as fruits, stem and root increments in the measurement of overall NPP. Please see section 3.1 (Lines 300-303) for the details of NPP measurement. To avoid confusion, we still remove the term “leaf NPP” and revise the sentence to “It needs to be noted that field measured NPP at the validation sites (section 3.1) does not consider the growing size of canopy (i.e. increasing LAI) which could partly explain the lower observed than simulated NPP at most sites”. (Lines 493-496)

9. Line 499, even temperature does not change much during the year in Indonesia, can radiation influence yield? Or does the simulated yield only response to precipitation?

**Answer 9:** It is true that temperature has little fluctuation in Indonesia. It mainly controls phenology via the accumulative heat index and GDD parameters. Radiation is indeed an important variable that drives yield as well as vegetative growth because it is involved in the radiative transfer and photosynthesis related processes in the whole CLM model. However, a simple linear correlation test shows that radiation (accumulative energy in the fruit-filling period) has a negative correlation with yield (Pearson's  $r = -0.28$ ,  $p\text{-value} < 1\text{E-}06$ ). We also perform a multiple regression including precipitation and solar radiation as well as their interaction as predictor variables, which are all significant in the fitted model:  $\text{Yield} = 84 - 0.05 \text{ Precipitation} - 0.09 \text{ Radiation} + 0.0001 \text{ Precipitation} \times \text{Radiation}$  ( $p\text{-values} < 1\text{E-}04$  for all the variables including the interaction term). Precipitation already exhibits strong positive influence on yield (see answer to comment 7). Thus the analyses suggest that the negative influence of radiation is mainly the outcome of the interaction between precipitation and radiation which themselves are negatively associated.

Given that radiation and precipitation as well as temperature are all key atmospheric forcing parameters used by the CLM-Palm model, their influence on yield is the combined outcome of different processes in phenology, allocation, radiative transfer, photosynthesis and stomatal conductance, etc. which are operating in different submodules. Therefore, it is difficult to interpret their individual influence on yield using simple statistical analysis.

We consider it is preferable not to discuss too much into these processes, otherwise the focus of this study, that is model development, calibration and validation on phenology and allocation, will be deviated. Thus, we only show the correlation and regression analyses on radiation here but not in the paper. To clarify the role of precipitation in the existing results

we add in the discussion that: “The seasonal variability in simulated yield corresponds to the precipitation data which is involved in the coupled stomatal conductance and photosynthesis and other hydrological processes in the model.” (Lines 511-513)

**Additional minor changes:**

1. We sent an email to the editor Dr. Lo on Oct. 1<sup>st</sup> 2015 to clarify a minor mistake on the color scales of Fig. 5, where the lower part (2003-2004) used a different scale from the upper part (2013-2014), making the LAI appear higher (more red) in 2003-2004 than they should be. The reason was found that the two parts were drawn separately but used the default settings that scaled the colors based on the distinct data ranges of each part. We double-checked the model output. The simulated phytomer LAI in 2003-2004 is only 0.043 at the maximum ( $< 0.14$  for 2013-2014), but it matches very well with the leaf samples we took on a young palm (the triangle mark in 2004). Now we corrected the figure using the same color scale (same data range) for the two parts so that they are consistent with the shared legend at the top of Fig.5. The lower part becomes much bluer that matches field data. It won't affect the way of interpretation in the results section. We only changed two sentences to include the simulated phytomer LAI values (Lines 415-418), and also add one sentence in figure 5's caption to clarify the meaning of phytomer in the model.
2. Acknowledgements to the reviewers are added: We also thank three anonymous reviewers for their constructive comments during the discussion and revision phases.

A sub-canopy structure for simulating oil palm in the Community Land Model (CLM-Palm):  
phenology, allocation and yield

Yuanchao Fan<sup>1,2,\*</sup>, Olivier Roupsard<sup>3,4</sup>, Martial Bernoux<sup>5</sup>, Gueric Le Maire<sup>3</sup>, Oleg Panferov<sup>6</sup>,  
Martyna M. Kotowska<sup>7</sup>, Alexander Knohl<sup>1</sup>

<sup>1</sup> University of Göttingen, Department of Bioclimatology, Büsgenweg 2, 37077 Göttingen, Germany

<sup>2</sup> AgroParisTech, SIBAGHE (Systèmes intégrés en Biologie, Agronomie, Géosciences, Hydrosiences et Environnement), 34093 Montpellier, France

<sup>3</sup> CIRAD, UMR Eco&Sols (Ecologie Fonctionnelle & Biogéochimie des Sols et des Agro-écosystèmes), 34060 Montpellier, France

<sup>4</sup> CATIE (Tropical Agricultural Centre for Research and Higher Education), 7170 Turrialba, Costa Rica

<sup>5</sup> IRD, UMR Eco&Sols, 34060 Montpellier, France

<sup>6</sup> University of Applied Sciences Bingen, 55411 Bingen am Rhein, Germany

<sup>7</sup> University of Göttingen, Department of Plant Ecology and Ecosystems Research, Untere Karspüle 2, 37073 Göttingen, Germany

\*Correspondence author. E-mail: yfan1@uni-goettingen.de

**Abstract:** In order to quantify the effects of forests to oil palm conversion occurring in the tropics on land-atmosphere carbon, water and energy fluxes, we develop a new perennial crop sub-model CLM-Palm for simulating a palm plant functional type (PFT) within the framework of the Community Land Model (CLM4.5). CLM-Palm is tested here on oil palm only but is meant of generic interest for other palm crops (e.g. coconut). The oil palm has monopodial morphology and sequential phenology of around 40 stacked phytomers, each carrying a large leaf and a fruit bunch, forming a multilayer canopy. A sub-canopy phenological and physiological parameterization is thus introduced, so that each phytomer has its own prognostic leaf growth and fruit yield capacity but with shared stem and root components. Phenology and carbon and nitrogen allocation operate on the different phytomers in parallel but at unsynchronized steps, separated by a thermal period. An important phenological phase is identified for the oil palm - the storage growth period of bud and “spear” leaves which are photosynthetically inactive before expansion. Agricultural practices such as transplanting, fertilization, and leaf pruning are represented. Parameters introduced for the oil palm were calibrated and validated with field measurements of leaf area index (LAI), yield and net primary production (NPP) from Sumatra, Indonesia. In calibration with a mature oil palm plantation, the cumulative yields from 2005 to 2014 matched notably well between simulation and observation (mean percentage error = 3%). Simulated inter-annual dynamics of PFT-level and phytomer-level LAI were both within the range of field measurements. Validation from eight independent oil palm sites shows the ability of the model to adequately predict the average leaf growth and fruit yield across sites and sufficiently represent the significant nitrogen and age related site-to-site variability in NPP and yield. Results also indicate that seasonal dynamics of yield and remaining small-scale site-to-site variability of NPP are driven by processes not yet implemented in the model or reflected in the input data. The new sub-canopy structure and phenology and allocation functions in CLM-Palm allow exploring the effects of tropical land use change, from natural ecosystems to oil palm plantations, on carbon, water and energy cycles and regional climate.

## 1. Introduction

Land-use changes in Southeast Asia have been accelerated by economy-driven expansion of oil palm (*Elaeis guineensis*) agriculture since the 1990s (Miettinen et al., 2011). Oil palm is currently one of the most rapidly expanding and high-yielding crops in the world (Carrasco et al., 2014) ~~and~~. In 2013 the harvested area of oil palm plantations in Indonesia alone was 7.1 million ha, accounting for 42% of world total (17 million ha), followed by Malaysia's 4.5 million ha (FAO, 2013). Indonesia's consistently high growth rate of oil palm area (nearly 10% annually; Gunarso et al. 2013) in the last two decades has placed it as the largest global palm-oil producer, and yet it has planned to double its oil-palm planted area from 9.7 million ha in 2009 to 18 million ha by 2020 (Koh and Ghazoul, 2010). Since oil palms favor a tropical-humid climate with consistently high temperatures and humidity, the plantations have converted large areas of rainforest in Indonesia ~~in the past two decades~~ including those on carbon-rich peat soils (Carlson et al., 2012; ~~Gunarso et al. 2013~~).

Undisturbed forests have long-lasting capacity to store carbon (C) in comparison to disturbed or managed vegetation (Luyssaert et al., 2008). Tropical forest to oil palm conversion has significant implications on above- and belowground ~~carbon~~C stocks (Kotowska et al., 2015a). However, the exact quantification of long-term and large-scale forest – oil palm replacement effects is difficult as the greenhouse gas balance of oil palms is still uncertain due to incomplete monitoring of the dynamics of oil palm plantations (including young development stage), and lack of understanding of the ~~carbon~~C, nitrogen (N), water and energy exchange between oil palms, soil and the atmosphere at ecosystem scale. Besides that, the assessment of these processes in agricultural ecosystems is complicated by human activities e.g. crop management, including planting and pruning, irrigation and fertilization, litter and residues management, and yield outputs. One of the suitable tools for evaluating the feedback of oil palm expansion is ecosystem modeling. Although a series of agricultural models exist for simulating the growth and yield of oil palm such as OPSIM (van Kraalingen et al., 1989),

ECOPALM (Combres et al., 2013), APSIM-Oil Palm (Huth et al., 2014), PALMSIM (Hoffmann et al., 2014), these models did not aim yet at the full picture of ~~carbon~~C, water and energy exchanges between land and atmosphere and remain to be coupled with climate models. Given the current and potential large-scale deforestation driven by the expansion of oil palm plantations, the ecosystem services such as yield, ~~carbon~~C sequestration, microclimate, energy and water balance of this new managed monoculture landscape have to be evaluated in order to estimate the overall impact of land-use change on environment including regional and global climate.

Land surface modeling has been widely used to characterize the two-way interactions between climate and human activities in terrestrial ecosystems such as deforestation, agricultural expansion, and urbanization (Jin and Miller, 2011; Oleson et al., 2004). A variety of land models have been adapted to simulate land-atmosphere energy and matter exchanges for major crops such as the Community Land Model (CLM, Oleson et al., 2013). CLM represents the crop and naturally vegetated land units as patches of plant functional types (PFTs) defined by their key ecological functions (Bonan et al., 2002). However, most of the crops being simulated are annual crops such as wheat, corn, soybean, etc. Their phenological cycles are usually represented as three stages of development from planting to leaf emergence, to fruit-fill and to harvest, all within a year. Attempts were also made to evaluate the climate effects of perennial deciduous crops, e.g. by extending the annual growing season ~~of~~ annuals to simulate earlier green-up and lagged senescence (Georgescu et al., 2011). However, the perennial evergreen crops such as oil palm, cacao, coffee, rubber, coconut, ~~and other~~ fruiting trees etc. and their long-term biophysical processes are not represented in the above land models yet, despite the worldwide growing demand (FAO, 2013).

Oil palm is a perennial evergreen crop which can be described by the Corner's architectural model (Hall et al., 1978). A number of phytomers, each carrying a large leaf (frond) and axillating a fruit bunch, emerge successively (nearly two per month) from a single meristem



(the bud) at the top of a solitary stem. They form a multilayer canopy with old leaves progressively being covered by new ones, until being pruned at senescence. Each phytomer has its own phenological stage and yield, according to respective position in the crown. The oil palm is productive for more than 25 years, including a juvenile stage of around 2 years. In order to capture the inter- and intra-annual dynamics of growth and yield and land-atmosphere energy, water and ~~earbon~~C fluxes in the oil palm system, a new structure and dimension detailing the phytomer-level phenology, ~~earbon~~(C) and ~~nitrogen~~(N) allocation and agricultural managements have to be added to the current integrated plant-level physiological parameterizations in the land models. This specific refinement needs to remain compliant with the current model structure though, and be simple to parameterize.

In this ~~context~~study, we develop a new CLM-Palm sub-model for simulating the growth, yield, and energy and material cycling of oil palm within the framework of CLM4.5. It introduces a sub-canopy phenological and physiological parameterization, so that multiple leaf and fruit components operate in parallel but at delayed steps. A phytomer in the model is meant to represent the average condition of an age-cohort of actual oil palm phytomers across the whole plantation landscape. The overall gross primary production (GPP) by leaves and ~~earbon~~C output by fruit harvests rely on the development trends of individual phytomers. The functions implemented for oil palm combine the characteristics of both trees and crops, such as the woody-like stem growth and turnover but the crop-like vegetative and reproductive allocations which enable fruit C and N output. Agricultural practices such as transplanting, fertilization, and leaf pruning are also represented.

The main objectives of this paper are to: i) describe the development of CLM-Palm including its phenology, ~~earbon~~C and ~~nitrogen~~N allocation, and yield output; ii) optimize model parameters using field-measured leaf area index (LAI) and observed long-term monthly yield data from a mature oil palm plantation in Sumatra, Indonesia; and iii) validate the model

against independent LAI, yield and net primary production (NPP) data from eight oil palm plantations of different age in Sumatra, Indonesia.

## 2. Model development

For adequate description of oil palm functioning, we adapted the CLM crop phenology, allocation and vegetative structure subroutines to the monopodial morphology and sequential phenology of oil palm so that each phytomer evolves independently in growth and yield (Fig. 1). Their phenology sequence is determined by the phyllochron (the period in thermal time between initiations of two subsequent phytomers) (Table A1). A maximum of 40 phytomers with expanded leaves, each growing up to 7-m long, are usually maintained in plantations by pruning management. There are also around 60 initiated phytomers developing slowly inside the bud. The largest ones, already emerged at the top of the crown but unexpanded yet, are named “spear” leaves (Fig. 1a). Each phytomer can be considered a sub-PFT component that has its own prognostic leaf growth and fruit yield capacity but having 1) the stem and root components that are shared by all phytomers, 2) the soil water content, ~~nitrogen~~N resources, and resulting photosynthetic assimilates that are also shared and partitioned among all phytomers, and 3) a vertical structure of the foliage, with the youngest at the top and the oldest at the bottom of the canopy. Within a phytomer the fruit and leaf components do not compete for growth allocation because leaf growth usually finishes well before fruit-fill starts. However one phytomer could impact the other ones through competition for assimilates, which is controlled by the C and N allocation subroutine according to their respective phenological stages.

Here we describe only the new phenology, allocation and agricultural management functions developed for the oil palm. Photosynthesis, respiration, water and ~~nitrogen~~N cycles and other biophysical processes already implemented in CLM4.5 (Oleson et al., 2013) are not modified (except N retranslocation scheme) for the current study. The following diagram shows the

new functions and their coupling with existing modules within the CLM4.5 framework (Fig. 2).

## 2.1. Phenology

Establishment of the oil palm plantation is implemented with two options: seed sowing or transplanting of seedlings. In this study, the transplanting option is used. We design 7 post-planting phenological steps for the development of each phytomer: 1) leaf initiation; 2) start of leaf expansion; 3) leaf maturity; 4) start of fruit-fill; 5) fruit maturity and harvest; 6) start of leaf senescence; and 7) end of leaf senescence and pruning (Fig. 1b). The first two steps differentiate pre-expansion (heterotrophic) and post-expansion (autotrophic) leaf growth phases. The other steps control leaf and fruit developments independently so that leaf growth and maturity could be finished well before fruit-fill and leaf senescence could happen after fruit harvest according to field observations. The modified phenology subroutine controls the life cycle of each phytomer (sub-PFT level) as well as the planting, stem and root turnover, vegetative maturity (start of fruiting) and final rotation (replanting) of the whole plant (PFT level). Detailed description of oil palm phenology and ~~nitrogen~~N retranslocation during senescence is in the Supplementary materials. The main phenological parameters are in Table A1.

All phytomers are assumed to follow the same phenological steps, where the thermal length for each phase is measured by growing degree-days (GDD; White et al., 1997). For oil palm, a new GDD variable with 15 °C base temperature and 25 degree-days daily maximum (Corley and Tinker, 2003; Goh, 2000; Hormaza et al., 2012) is accumulated from planting (abbr. GDD<sub>15</sub>). The phenological phases are signaled by respective GDD requirements, except that pruning is controlled by the maximum number of expanded phytomers according to plantation management (Table A1). Other processes in the model such as ~~carbon~~C and ~~nitrogen~~N allocation for growth of new tissues respond to this phenology scheme at both PFT level and phytomer level.

## 2.2. CarbonC and NitrogenN allocation

In CLM, the fate of newly assimilated carbonC from photosynthesis is determined by a coupled C and N allocation routine. Potential allocation for new growth of various plant tissues is calculated based on allocation coefficients and their allometric relationship (Table A2).

A two-step allocation scheme is designed for the sub-canopy phytomer structure and according to the new phenology. First, available C (after subtracting respiration costs) is partitioned to the root, stem, overall leaf, and overall fruit pools with respect to their relative demands by dynamic allocation functions according to PFT-level phenology. The C:N ratios for different tissues link C demand and N demand so that a N down-regulation mechanism is enabled to rescale GPP and C allocation if N availability from soil mineral N pool and retranslocated N pool does not meet the demand. Then, the actual C and N allocated to the overall leaf or fruit pools are partitioned between different phytomers at the sub-PFT level (Fig. 2). Details are described below.

### 2.2.1. PFT level allocation

C and N allocation at the PFT level is treated distinctly before and after oil palm reaches vegetative maturity. At the juvenile stage before fruiting starts (i.e.  $GDD_{15} < GDD_{min}$ ) all the allocation goes to the vegetative components. The following equations are used to calculate the allometric ratios for partitioning available C and N to the leaf, stem, and root pools.

$$A_{root} = a_{root}^i - (a_{root}^i - a_{root}^f) \frac{DPP}{Age_{max}}, \quad (\text{Eq. 1})$$

$$A_{leaf} = f_{leaf}^i \times (1 - A_{root}) \quad (\text{Eq. 2})$$

$$A_{stem} = 1 - A_{root} - A_{leaf} \quad (\text{Eq. 3})$$

where  $\frac{DPP}{Age_{max}} \leq 1$ ,  $DPP$  is the days past planting, and  $Age_{max}$  is the maximum plantation age (~25 years).  $a_{root}^i$  and  $a_{root}^f$  are the initial and final allocation coefficients for roots and  $f_{leaf}^i$  is the initial leaf allocation coefficient before fruiting (Table A2). Root and stem allocation ratios are calculated with Eqs. 1 and 3 for all ages and phenological stages of oil palm.

After fruiting begins, the new non-linear function is used for leaf allocation:

$$A_{leaf} = a_{leaf}^2 - (a_{leaf}^2 - a_{leaf}^f) \left( \frac{DPP - DPP_2}{Age_{max} \times d_{mat} - DPP_2} \right)^{d_{alloc}^{leaf}} \quad (\text{Eq. 4})$$

where  $a_{leaf}^2$  equals the last value of  $A_{leaf}$  calculated right before fruit-fill starts and  $DPP_2$  is the days past planting right before fruit-fill starts.  $d_{mat}$  controls the age when the leaf allocation ratio approaches its final value  $a_{leaf}^f$ , while  $d_{alloc}^{leaf}$  determines the shape of change (convex when  $d_{alloc}^{leaf} < 1$ ; concave when  $d_{alloc}^{leaf} > 1$ ).  $A_{leaf}$  stabilizes at  $a_{leaf}^f$  when  $DPP \geq Age_{max} d_{mat}$ . The equations reflect changed vegetative allocation strategy that shifts resources to leaf for maintaining LAI and increasing photosynthetic productivity when fruiting starts. The three vegetative allocation ratios  $A_{leaf}$ ,  $A_{stem}$  and  $A_{root}$  always sum to 1.

At the reproductive phase a fruit allocation ratio  $A_{fruit}$  is introduced, which is relative to the total vegetative allocation unity. To represent the dynamics of reproductive allocation effort of oil palm, we adapt the stem allocation scheme for woody PFTs in CLM, in which increasing NPP results in increased allocation ratio for the stem wood (Oleson et al., 2013). A similar formula is used for reproductive allocation of oil palm so that it increases with increasing NPP:

$$A_{fruit} = \frac{2}{1 + e^{-b(NPP_{mon} - 100)}} - a \quad (\text{Eq. 5})$$

where  $NPP_{mon}$  is the monthly sum of NPP from the previous month calculated with a run-time accumulator in the model. The number 100 ( $\text{g C m}^{-2} \text{ mon}^{-1}$ ) is the base monthly NPP

when the palm starts to yield (Kotowska et al., 2015a). Parameters  $a$  and  $b$  adjust the base allocation rate and the slope of change, respectively (Table A2). This function generates a dynamic curve of  $A_{fruit}$  increasing from the beginning of fruiting to full vegetative maturity, which is used in the allocation allometry to partition assimilates between vegetative and reproductive pools (Fig. 3).

#### 2.2.2. Sub-PFT (phytomer) level allocation

Total leaf and fruit allocations are partitioned to the different phytomers according to their phenological stages. Fruit allocation per phytomer is calculated with a sink size index:

$$S_p^{fruit} = \frac{GDD_{15} - H_p^{F.fill}}{H_p^{F.mat} - H_p^{F.fill}}, \quad (\text{Eq. 6})$$

where  $p$  stands for the phytomer number,  $H_p^{F.fill}$  and  $H_p^{F.mat}$  are the phenological indices for the start of fruit-fill and fruit maturity (with  $H_p^{F.fill} \leq GDD_{15} \leq H_p^{F.mat}$ ).  $S_p^{fruit}$  increases from zero at the beginning of fruit-fill to the maximum of 1 right before harvest for each phytomer. This is because the oil palm fruit accumulates assimilates at increasing rate during development until the peak when it becomes ripe and oil synthesis dominates the demand (Corley and Tinker, 2003). The sum of  $S_p^{fruit}$  for all phytomers gives the total reproductive

sink size index. Each phytomer receives a portion of fruit allocation by  $\frac{S_p^{fruit}}{\sum_{p=1}^n S_p^{fruit}} \times A_{fruit}$ ,

where  $A_{fruit}$  is the overall fruit allocation by Eq. 5.

An important allocation strategy for leaf is the division of displayed versus storage pools for the pre-expansion and post-expansion leaf growth phases. These two types of leaf C and N pools are distinct in that only the displayed pools contribute to LAI growth, whereas the storage pools support the growth of unexpanded phytomers, i.e. bud & spear leaves, which remain photosynthetically inactive. Total C and N allocation to the overall leaf pool is divided

to the displayed and storage pools by a fraction  $lf_{disp}$  (Table A2) according to the following equation:

$$\begin{aligned} A_{leaf}^{display} &= lf_{disp} \times A_{leaf} \\ A_{leaf}^{storage} &= (1 - lf_{disp}) \times A_{leaf} \end{aligned} \quad (\text{Eq. 7})$$

The plant level  $A_{leaf}^{display}$  and  $A_{leaf}^{storage}$  are then distributed evenly to expanded and unexpanded phytomers, respectively, at each time step. When a phytomer enters the leaf expansion phase, C and N from its leaf storage pools transfer gradually to the displayed pools during the expansion period. Therefore, a transfer flux is added to the real-time allocation flux and they together contribute to the post-expansion leaf growth.

LAI is calculated only for each expanded phytomer according to a constant specific leaf area (SLA) and prognostic amount of leaf C accumulated by phytomer  $n$ . In case it reaches the prescribed maximum ( $PLAI_{max}$ ), partitioning of leaf C and N allocation to this phytomer becomes zero.

### 2.3. Other parameterizations

~~Nitrogen~~N retranslocation is performed exclusively during leaf senescence and stem turnover. A part of N from senescent leaves and from the portion of live stem that turns dead is remobilized to a separate N pool that feeds plant growth or reproductive demand. ~~Nitrogen~~N of fine roots is all moved to the litter pool during root turnover. We do not consider N retranslocation from live leaves, stem and roots specifically during grain-fill that is designed for annual crops (Drewniak et al., 2013) because oil palm has continuous fruit-fill year around at different phytomers.

The fertilization scheme for oil palm is adapted to the plantation management generally carried out in our study area, which applies fertilizer biannually, starting only 6 years after planting, assuming each fertilization event lasts one day. Currently the CLM-CN

belowground routine uses an unrealistically high denitrification rate under conditions of ~~nitrogen~~N saturation, e.g. after fertilization, which results in a 50% loss of any excess soil mineral ~~nitrogen~~N per day (Oleson et al., 2013). This caused the simple biannual regular fertilization nearly useless because peak N demand by oil palm is hard to predict given its continuous fruiting and vegetative growth and most fertilized N is thus lost in several days. The high denitrification factor has been recognized as an artifact (Drewniak et al., 2013; Tang et al., 2013). According to a study on a banana plantation in the tropics (Veldkamp and Keller, 1997), around 8.5% of fertilized N is lost as nitrogen oxide (N<sub>2</sub>O and NO). Accounting additionally for a larger amount of denitrification loss to gaseous N<sub>2</sub>, we modified the daily denitrification rate from 0.5 to 0.001, which gives a 30% annual loss of N due to denitrification that matches global observations (Galloway et al., 2004).

The irrigation option is turned off because oil palm plantations in the study area are usually not irrigated. Other input parameters for oil palm such as its optical, morphological, and physiological characteristics are summarized in Table A3. Most of them are generalized over the life of oil palm.

### **3. Model evaluation**

#### **3.1. Site data**

Two oil palm plantations in the Jambi province of Sumatra, Indonesia provide data for calibration. One is a mature industrial plantation at PTPN-VI (01 °41.6' S, 103 °23.5' E, 2186 ha) planted in 2002, which provides long-term monthly harvest data (2005 to 2014). Another is a 2-year young plantation at a nearby smallholder site Pompa Air (01 °50.1' S, 103 °17.7' E, 5.7 ha). The leaf area and dry weight at multiple growth stages were measured by sampling leaflets of phytomers at different ranks (+1 to +20) on a palm and repeating for 3 different ages within the two plantations. The input parameter SLA (Table A2) was derived from leaf area and dry weight (excluding the heavy rachis). The phytomer-level LAI was estimated



based on the number of leaflets (90-300) per leaf of a certain rank and the PFT-level LAI was estimated by the number of expanded leaves (35-45) per palm of a certain age. In both cases, a planting density of 156 palms per hectare (8m × 8m per palm) was used according to observation.

Additionally, LAI, yield and NPP measurements from eight independent smallholder oil palm plantations (50m × 50m each) were used for model validation (Table 1). Four of these sites (HO1, HO2, HO3, HO4, ~~11-18 years old~~) are located in the Harapan region nearby PTPN-VI, and another four (BO2, BO3, BO4, BO5, ~~10-14 years old~~) are in Bukit Duabelas region (02°04' S, 102°47' E), both in Jambi, Sumatra. Fresh bunch harvest data were collected at these sites for a whole year in 2014. Harvest records from both PTPN-VI and the 8 validation sites were converted to harvested ~~carbon~~C (g C/m<sup>2</sup>) with mean wet/dry weight ratio of 58.65 % and C content 60.13 % per dry weight according to C:N analysis (Kotowska et al., 2015a). The oil palm monthly NPP and its partitioning between fruit, leaf, stem and root were estimated based on measurements of fruit yield (monthly), pruned leaves (monthly), stem increment (every 6 month) and fine root samples (once in a interval of 6-8 month) at the eight validation sites (Kotowska et al., 2015b).

The amount of fertilization at the industrial plantation PTPN-VI was 456 kg N ha<sup>-1</sup> yr<sup>-1</sup>, applied regularly twice per year since 6-year old. The smallholder plantations in Harapan (H plots) and Bukit Duabelas (B plots) used much less fertilizer. From interview data, the H plots had roughly regular N fertilization (twice per year), whereas among the B plots only BO3 indicated one fertilization event per year but the amount was unclear (applied chicken manure in 2013) and the other plots had no N fertilization in 2013 and 2014 due to financial difficulty. Fertilization history prior to 2013 is unavailable for all the smallholder plantations. Given the limited information, we consider two levels of fertilization for H plots (regular: 96 kg N ha<sup>-1</sup> yr<sup>-1</sup>, from 6-year old until 2014) and B plots (reduced: 24 kg N ha<sup>-1</sup> yr<sup>-1</sup>, from 6-year old until 2012), respectively (Table 1).

The mean annual rainfall (the Worldclim database: <http://www.worldclim.org> (Hijmans et al., 2005); average of 50 years) of the two investigated landscapes in Jambi Province was ~2567 mm y<sup>-1</sup> in the Harapan region (including PTPN-VI) and ~2902 mm y<sup>-1</sup> in the Bukit Duabelas region. In both areas, May to September represented a markedly drier season (30% less precipitation) in comparison to the rainy season between October and April. Air temperature is relatively constant throughout the year with an annual average of 26.7 °C. In both landscapes, the principal soil types are Acrisols: in the Harapan landscape loam Acrisols dominate, whereas in Bukit Duabelas the majority is clay Acrisol. Soil texture such as sand/silt/clay ratios and soil organic matter C content were measured at multiply soil layers (down to 2.5m) (Allen et al., 2015). They were used to create two sets of surface input data for the two regions separately.

### **3.2. Model setup**

The model modifications and parameterizations were implemented according to CLM4.5 standards. A new sub-PFT dimension called *phytomer* was added to all the new variables so that the model can output history tapes of their values for each phytomer and prepare restart files for model stop and restart with bit-for-bit continuity. Simulations were set up in point mode (a single 0.5×0.5 degree grid) at every 30-min time step. A spin-up procedure (Koven et al., 2013) was followed to get a steady-state estimate of soil C and N pools, with the CLM-CN decomposition cascade and broadleaf evergreen tropical forest PFT. The soil C and N pools were rescaled to match the average field observation at two reference lowland rainforest sites in Harapan and Bukit Duabelas regions (Allen et al., 2015; Guillaume et al., 2015), which serve as the initial conditions. The forest was replaced with the oil palm at a specific year of plantation establishment (2002 for PTPN-VI and 1996, 1997, 1999, 2000, 2001, 2002, 2003, 2004 for HO3, HO1, HO2, BO2, BO3, BO4, HO4, BO5, respectively). The oil palm functions were then turned on and simulations continued until 2014. The 3-hourly ERA Interim climate data (Dee et al., 2011) were used as atmospheric forcing.

### 3.3. Calibration of key parameters

A simulation from 2002 to 2014 at the PTPN-VI site was used for model calibration. Both the PFT level and phytomer level LAI development were calibrated with field observations in 2014 from a chronosequence approach (space for time substitution) using oil palm samples of three different age and multiple phytomers of different rank (section 3.1). Simulated yield outputs (around twice per month) were calibrated with monthly harvest records of PTPN-VI plantation from 2005 to 2014. Cumulative yields were compared because the timing of harvest in the plantations was largely uncertain and varied depending on weather and other conditions.

To simplify model calibration, we focused on parameters related to the new phenology and allocation processes. Phenological parameters listed in Table A1 were determined according to field observations and existing knowledge about oil palm growth phenology (Combres et al., 2013; Corley and Tinker, 2003) as well as plantation management in Sumatra, Indonesia. Allocation coefficients in Table A2 were more uncertain and they were the key parameters to optimize in order to match observed LAI and yield dynamics according to the following sensitivity analysis. Measurements of oil palm NPP and its partitioning between fruit, canopy, stem, and root from the eight sites (section 3.1) were used as a general reference when calibrating the allocation coefficients.

Leaf C:N ratio and *SLA* were determined by field measurements. Other C:N ratios and optical and morphological parameters in Table A3 were either fixed by field observations or adjusted in-between trees and crops.

### 3.4. Sensitivity analysis

Performing a full sensitivity analysis of all parameters used in simulating oil palm (more than 100 parameters, though a majority are shared with natural vegetation and other crops) would

be a challenging work. As with calibration, we limited the sensitivity analysis to a set of parameters introduced for the specific PFT and model structure designed for oil palm (Tables A1 and A2). Among the phenological parameters, *mxlivenp* (maximum number of expanded phytomers) and *phyllochron* (Table A1) are closely related to pruning frequency but they should not vary widely for a given oil palm breed and plantation condition. Therefore, they were fixed at the average level for the study sites in Jambi, Sumatra. Parameter  $PLAI_{max}$  is only meant for error controlling, although in our simulations phytomer-level LAI never reached  $PLAI_{max}$  (see Fig. 5 in results) because environmental constraints and ~~nitrogen~~N down-regulation already limited phytomer leaf growth well within the range.  $GDD_{init}$  was kept to zero because only the transplanting scenario was considered for seedling establishment.

We tested two hypotheses of phytomer level leaf development based on the other phenological parameters: 1) considering the leaf storage growth period, that is, the bud & spear leaf phase is explicitly simulated with the GDD parameters in Table A1 and  $lf_{disp} = 0.3$  in Table A2; 2) excluding the storage growth period by setting  $GDD_{exp} = 0$  and  $lf_{disp} = 1$  so that leaf expands immediately after initiation and leaf C and N allocation all goes to the photosynthetic active pools.

The sensitivity of allocation and photosynthesis parameters in Table A2 were tested by adding or subtracting 10% or 30% to the baseline values (calibrated) one-by-one and calculating their effect on final cumulative yield at the end of simulation (December 2014). In fact, all the allocation parameters are interconnected because they co-determine photosynthesis capacity and respiration costs as partitioning to the different vegetative and reproductive components varies. This simple approach provides a starting point to identify sensitive parameters, although a more sophisticated sensitivity analysis is needed in the future.

### 3.5. Validation

In this study, we only validated the model structure and model behavior on simulating aboveground C dynamics and partitioning as represented by LAI, fruit yield and NPP. Independent leaf measurement, yield and monthly NPP data collected in 2014 from the eight mature oil palm sites (H and B plots) were compared with the eight simulations using the same model settings and calibrated parameters, except that two categories of climate forcing, surface input data (for soil texture) and fertilization (regular vs. reduced) were prescribed for the H plots and B plots, respectively.

## **4. Results**

### **4.1. Calibration with LAI and yield**

In calibration with the industrial PTPN-VI plantation, the PFT-level LAI dynamics simulated by the model incorporating the pre-expansion phase matches well with the LAI measurements for three different ages (Fig. 4). Simulated LAI for the PFT increases with age in a sigmoid relationship. The dynamics of LAI is also impacted by pruning and harvest events because oil palms invest around half of their assimilates into fruit yield. Oil palms are routinely pruned by farmers to maintain the maximum number of expanded leaves around 40. Hence, when yield begins 2-3 years after planting, LAI recurrently shows an immediate drop after pruning and then quickly recovers. The pruning frequency decreases with age because the phyllochron increases to 1.5 times at 10-year old (Supplementary materials). Simulations without the pre-expansion storage growth phase show an unrealistic fast increase of LAI before 3 years old, much higher than observed in the field. At older age after yield begins, LAI drops drastically and recovers afterwards. Although the final LAI could stabilize at a similar level, the initial jump and drop of LAI at young stage do not match field observations and cannot be solved by adjusting parameters other than  $GDD_{exp}$ . Hereafter, all simulations were run using the pre-expansion phase.

The phytomer level LAI development is comparable with leaf samples from the field (Fig. 5). The two leaf samples at rank 5 (LAI = 0.085) and rank 20 (LAI = 0.122) of a mature oil palm in PTPN-VI (the two black triangles for 2014) are ~~within the range of~~ slightly lower than simulated values (0.089 and 0.138, respectively). The other sample at rank 25 (LAI = 0.04, for 2004) of a young oil palm in Pompa Air (~~smallholder plantation~~) is ~~lower~~ slightly higher than the simulated value (0.036). Each horizontal color bar clearly marks the post-expansion leaf phenology cycle, including gradual increment of photosynthetic LAI during phytomer development and gradual declining during senescence. The pre-expansion phase is not included in the figure but model outputs show that roughly 60-70% of leaf C in a phytomer is accumulated before leaf expansion, which is co-determined by the allocation ratio  $lf_{disp}$  and the lengths of two growth phases set by  $GDD_{exp}$  and  $GDD_{L.mat}$ . This is comparable to observations on coconut palm that dry mass of the oldest unexpanded leaf accounts for 60% of that of a mature leaf (Navarro et al., 2008). Only when the palm becomes mature, phytomer LAI could come closer to the prescribed  $PLAI_{max}$  (0.165). However, during the whole growth period from 2002 to 2014 none of the phytomers have reached  $PLAI_{max}$ , which is the prognostic result of the ~~carbon~~C balance simulated by the model.

The cumulative yield of baseline simulation has overall high consistency with harvest records (Fig. 6). The mean percentage error (MPE) is only 3%. The slope of simulated curve increases slightly after 2008 when the LAI continues to increase and NPP reaches a high level (Fig. 3). The harvest records also show the same pattern after 2008 when heavy fertilization began ( $456 \text{ kg N ha}^{-1} \text{ yr}^{-1}$ ).

The per-month harvest records exhibit strong zig-zag pattern (Fig. 7). One reason is that oil palms are harvested every 15-20 days and summarizing harvest events by calendar month would result in uneven harvest times per month, e.g. two harvests fall in a previous month and only one in the next month. Yet it still shows that harvests at PTPN-VI plantation dominated from October to December whereas in the earlier months of each year harvest amounts were

significantly lower. The simulated monthly yield has less seasonal fluctuation, but it ~~responds~~ corresponds to the ~~fluctuation-general pattern~~ of precipitation (Fig. 7). A significant slight positive linear correlation exists between simulated yield (detrended to minimize phenological effects) and the ~~mean-accumulative~~ precipitation of a ~~60~~120-day period (~~corresponds to~~ the main fruit-filling and oil synthesis period) before each harvest event (Pearson's  $r = -0.15$  0.32,  $p\text{-value} < 1\text{E-}06$ ). Examining the longer term year-to-year variability, a clear increasing trend of yield with increasing plantation age is captured by the model, largely matching field records since the plantation began to yield in 2005.

## 4.2. Sensitivity analysis

The leaf ~~nitrogen~~N fraction in Rubisco ( $F_{LNR}$ ) is shown to be the most sensitive parameter (Fig. 8), because it determines the maximum rate of carboxylation at 25 °C ( $V_{cmax25}$ ) together with  $SLA$  (also sensitive), foliage ~~nitrogen~~N concentration ( $CN_{leaf}$ , Table A3) and other constants. Given the fact that  $F_{LNR}$  should not vary widely in nature for a specific plant, we constrained this parameter within narrow boundaries to get a  $V_{cmax25}$  around 100.7, the same as that shared by all other crop PFTs in CLM. We fixed  $SLA$  to 0.013 by field measurements. The value is only representative of the photosynthetic leaflets. The initial root allocation ratio ( $a_{root}^i$ ) has considerable influence on yield because it modifies the overall respiration cost along the gradual declining trend of fine root growth across 25 years (Eq. 1). The final ratio ( $a_{root}^f$ ) has limited effects because its baseline value (0.1) is set very low and thus the percentage changes are insignificant. The leaf allocation coefficients ( $f_{leaf}^i$ ,  $a_{leaf}^f$ ) are very sensitive parameters because they determine the magnitudes of LAI and GPP and consequently yield. The coefficients  $d_{mat}$  and  $d_{alloc}^{leaf}$  control the nonlinear curve of leaf development (Eq. 4) and hence the dynamics of NPP and that partitioned to fruits. Increased  $F_{stem}^{live}$  results in higher proportion of live stem throughout life, given the fixed stem turnover rate (Supplementary materials), and therefore it brings higher respiration cost and lower yield. The relative influence of fruit allocation coefficients  $a$  and  $b$  on yield is much lower than the

leaf allocation coefficients because of the restriction of  $A_{fruit}$  by NPP dynamics (Eq. 5). Parameters  $lf_{disp}$  and  $transplant$  have negligible effects.  $lf_{disp}$  has to work together with the phenological parameter  $GDD_{exp}$  to give a reasonable size of spear leaves before expansion according to field observation. The sensitivity of  $GDD_{exp}$  is shown in Fig. 4. Varying the size of seedlings at transplanting by 10% or 30% does not alter the final yield, likely because the initial LAI is still within a limited range (0.1~0.2) given the baseline value 0.15.

### 4.3. Model validation with independent dataset

The LAI development curves for the eight oil palm sites follow similar patterns since field transplanting in different years, except that the B plots (BO2, BO3, BO4) are restrained in LAI growth after 11 years old because of reduced fertilization (Fig. 9a). The field data in 2014 also shows the check by N limitation and even exhibits a decreasing trend of LAI with increasing plantation age at B plots except BO5 which is under 10 years old (Fig. 9b). In general, the modelled LAI has a positive relationship with plantation age under regularly fertilized condition and it stabilizes after 15-year old (site HO3) as controlled by  $d_{mat}$  (Eq. 4). This age-dependent trend is observed in the field with a notable deviation by site HO1. The average LAI of the eight sites from the model is comparable with field measurement in 2014 (MPE = 13%). There are large uncertainties in field LAI estimates because we did not measure LAI at the plot level directly but only sampled leaf area and dry weight of individual phytomers and scaled the values up.

The simulated annual yields match closely with field observations in 2014 at both the H plots (MPE = 2%) and B plots (MPE = 2%; Fig. 10). With regular fertilization in the H plots, both the modelled and observed yield are slightly higher in the older plantations (HO2, HO1, and HO3) than the younger one (HO4) but stabilize around  $1280 \text{ g C m}^{-2} \text{ yr}^{-1}$  past the age of 15 years. In contrast, the B plots have significantly lower yield because of reduced N input and the model is able to capture the N limitation effect on both NPP and yield, i.e. the declining trend with increasing age, which is consistent with field observation. The model simulates



slightly higher NPP than field estimates at 7 smallholder sites (MPE = 10%) using the input parameters calibrated and optimized only for LAI and yield at the industrial PTPN-VI plantation. It needs to be noted that field measured leaf NPP only includes leaf litter production but at the validation sites (section 3.1) does not account for consider the growing size of canopy (i.e. increasing LAI) which could partly explain the lower observed than simulated NPP at most sites.

## 5. Discussion

Calibration and validation with multiple site data demonstrate the utility of CLM-Palm and its sub-canopy structure for simulating the growth and yield of the unique oil palm plantation system within a land surface modeling context.

The pre-expansion phenological phase is proved necessary for simulating both phytomer-level and PFT-level LAI development in a prognostic manner. The leaf C storage pool provides an efficient buffer to support phytomer development and maintain overall LAI during fruiting. It also avoids an abnormally fast increase of LAI in the juvenile stage when C and N allocation is dedicated to the vegetative components. Without the leaf storage pool, the plant's canopy develops unrealistically fast at young age and then enters an emergent drop once fruit-fill begins (Fig. 4). This is because the plant becomes unable to sustain leaf growth just from its current photosynthetic assimilates when a large portion is allocated to fruits.

The model well simulates year-to-year variability in yield (Fig. 7), in which the increasing trend is closely related to the fruit allocation function (Fig. 3) and LAI development (Fig. 4).

The seasonal variability in simulated yield corresponds to the precipitation data which is involved in the coupled stomatal conductance and photosynthesis and other hydrological processes in the model. but But it is difficult to interpret the difference with from monthly harvest records due to the artificial zig-zag pattern. The harvest records from plantations do not necessarily correspond to the amount of mature fruits along a phenological time scale due

to varying harvest arrangements, e.g. fruits are not necessarily harvested when they are ideal for harvest, but when it is convenient. Observations of mature fruits on a tree basis (e.g. Navarro et al., 2008 on coconut) would be more suitable to compare with modeled yield, but such data are not available at our sites. Some studies have also demonstrated important physiological mechanisms on oil palm yield including inflorescence gender determination and abortion rates that both respond to seasonal climatic dynamics although with a time lag (Combres et al., 2013; Legros et al., 2009). The lack of representation of such physiological traits might affect the seasonal dynamics of yield simulated by our model, but these mechanisms are rarely considered in a land surface modeling context. Nevertheless, the results correspond generally to the purpose of our modeling which is focused on the long-term climatological effects of oil palm agriculture. The correct representation of multi-year trend of ~~carbon~~C balance which we did reach is more important than the correct prediction of each yield. For latter the more agriculturally-oriented models should be used.

Resource allocation patterns for perennial crops are more difficult to simulate than annual crops. For annuals, the LAI is often assumed to decline during grain-fill (Levis et al., 2012). However, the oil palm has to sustain a rather stable leaf area while partitioning a significant amount of C to the fruits. The balance between reproductive and vegetative allocations is crucial. The dynamics of  $A_{fruit}$  as a function of monthly NPP is proved useful to capture the increasing yield capacity of oil palms during maturing at favorable conditions (Fig. 6, 7) and also able to adjust fruit allocation and shift resources to the vegetative components under stress conditions (e.g. N limitation, Fig. 9 and 10). The value of  $A_{fruit}$  increased from 0.5 to 1.5 (Fig. 3), resulting more than a half partitioning of NPP to the reproductive pool at mature stage which matched closely with field observations (Fig. 10; Kotowska et al., 2015a; Kotowska et al., 2015b). Our experiments (not shown here) confirmed that the dynamic function is more robust than a simple time-dependent or vegetation-size-dependent allocation function.

The phenology and allocation processes in land surface models are usually aimed to represent the average growth trend of a PFT at large spatial scale (Bonan et al., 2002; Drewniak et al., 2013). We made a step forward by comparing point simulations with multiple specific site observations. The model predicts well the average LAI development and yield as well as NPP of mature plantations across two different regions. Site-to-site variability in yield and NPP at the Harapan and Bukit Duabelas plots under contrasting conditions (regular vs. reduced fertilization) is largely captured by the model. The decreasing trend of yield and pause of LAI growth in B plots after 10 years old (Fig. 9, 10) reflect reduced N availability observed in the clay Acrisol soil in Bukit Duabelas (Allen et al., 2015) with very limited C and N return from leaf litter because of the pruning and piling of highly lignified leaves (Guillaume et al., 2015). Yet there remains small-scale discrepancy in LAI, NPP or yield in some sites which is possibly due to the fact that microclimate, surface input data and the amount and timing of fertilization were only prescribed as two categories for H and P plots, respectively. Field data show the proportion of NPP allocated to yield is significantly higher in plot HO1 (70%) than in other plots (50% to 65%) which could explain the low LAI of HO1. This is not reflected in the model as the same parameters are used in the fruit allocation function (Eq. 5) across sites. The deviation in allocation pattern is likely due to differences in plantation management (e.g. harvest and pruning cycles), which has been shown to be crucial for determining vegetative and reproductive growth (Euler et al., 2015). Other factors such as insects, fungal infection, and possibly different oil palm progenies could also result in difference in oil palm growth and productivity, but they are typically omitted in land surface models. Generalized input parameterization across a region is usually the case when modeling with a PFT, although a more complex management scheme (e.g. dynamic fertilization) could be devised and evaluated thoroughly with additional field data, which we lack at the moment.

Overall, the sub-canopy phytomer-based structure, the extended phenological phases for a perennial crop PFT and the two-step allocation scheme of CLM-Palm are distinct from existing functions in land surface models. The phytomer configuration is similar to the one

already implemented in other oil palm growth and yield models such as the APSIM-Oil Palm model (Huth et al., 2014) or the ECOPALM yield prediction model (Combres et al., 2013). But the implementation of this sub-canopy structure is the first attempt among land surface models. CLM-Palm incorporates the ability of an agricultural model for simulating growth and yield, beside that it allows the modeling of biophysical and biogeochemical processes as a land model should do, e.g. what is the whole fate of ~~earbon~~C in plant, soil and atmosphere if land surface composition shifts from a natural system to the managed oil palm system? In a following study, a fuller picture of the ~~earbon~~C, ~~nitrogen~~N, water and energy fluxes over the oil palm landscape are examined with CLM-Palm presented here and evaluated with Eddy Covariance flux observation data. We develop this palm sub-model in the CLM framework as it allows coupling with climate models so that the feedbacks of oil palm expansion to climate can be simulated in future steps.

## 6. Conclusions

The development of CLM-Palm including canopy structure, phenology, and ~~earbon~~C and ~~nitrogen~~N allocation functions was proposed for modeling an important agricultural system in the tropics. This paper demonstrates the ability of the new palm module to simulate the inter-annual dynamics of vegetative growth and fruit yield from field planting to full maturity of the plantation. The sub-canopy-scale phenology and allocation strategy are necessary for this perennial evergreen crop which yields continuously on multiple phytomers. The pre-expansion leaf storage growth phase is proved essential for buffering and balancing overall vegetative and reproductive growth. Average LAI, yield and NPP are satisfactorily simulated for multiple sites, which fulfills the main mission of a land surface modeling approach, that is, to represent the average conditions and dynamics of large-scale processes. On the other hand, simulating small-scale site-to-site variation (50m × 50m sites) requires detailed input data on site conditions (e.g. microclimate) and plantation managements that are often not available thus limiting the applicability of the model at small scale. Nevertheless, the CLM-Palm model sufficiently represents the significant region-wide variability in oil palm NPP and yield driven

by nutrient input and plantation age in Jambi, Sumatra. The point simulations here provide a starting point for calibration and validation at large scales.

To be run in a regional or global grid, the age class structure of plantations needs to be taken into account. This can be achieved by setting multiple replicates of the PFT for oil palm, each planted at a point of time at a certain grid. As a result, a series of oil palm cohorts developing at different grids could be configured with a transient PFT distribution dataset, which allows for a quantitative analysis of the effects of land-use changes, specifically rainforest to oil palm conversion, on ~~carbon~~C, water and energy fluxes. This will contribute to the land surface modeling community for simulating this structurally unique, economically and ecologically sensitive, and fast expanding oil palm land cover.

#### **Acknowledgements:**

This study was funded by the European Commission Erasmus Mundus FONASO Doctorate fellowship. Field trips were partly supported by the Collaborative Research Centre 990 (Ecological and Socioeconomic Functions of Tropical Lowland Rainforest Transformation Systems (Sumatra, Indonesia)) funded by the German Research Foundation (DFG). We are grateful to Kara Allen (University of Göttingen, Germany), Dr. Bambang Irawan (University of Jambi, Indonesia) and the PTPN-VI plantation in Jambi for providing field data on oil palm. The source code of the post-4.5 version CLM model was provided by Dr. Samuel Levis from National Center for Atmospheric Research (NCAR), Boulder, CO, USA. We also thank three anonymous reviewers for their constructive comments during the open discussion and revision phases.

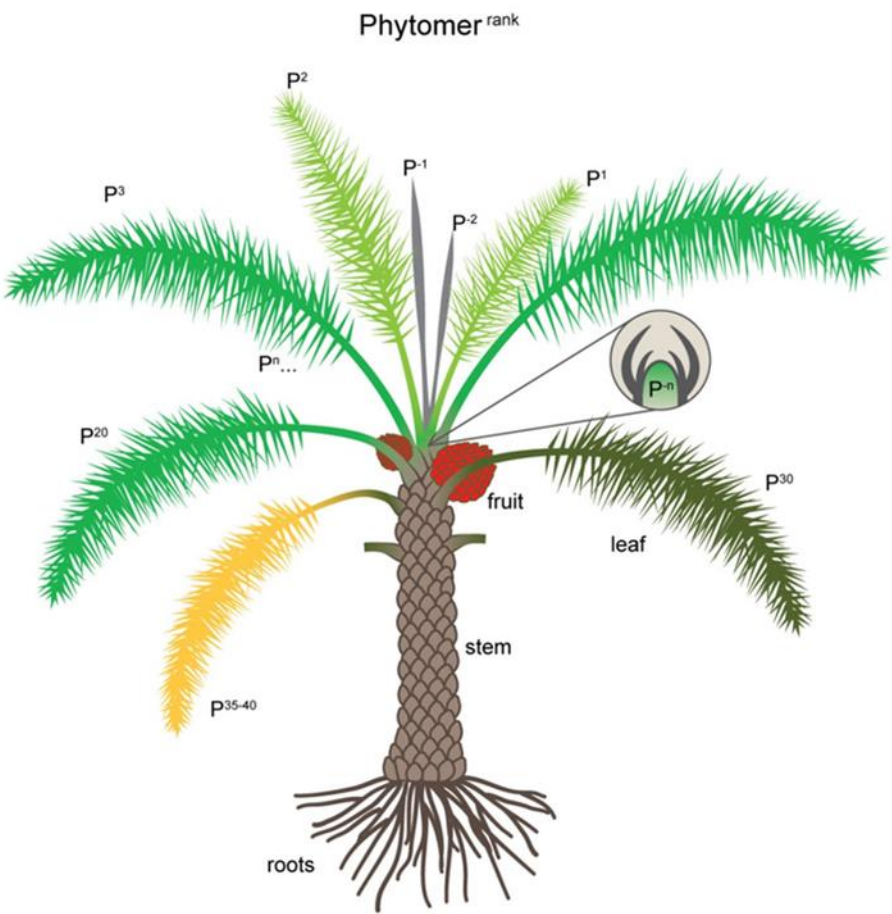
This open-access publication was funded by the University of Göttingen.

## Tables

Table 1. Site conditions and N fertilization records at the calibration and validation plots.

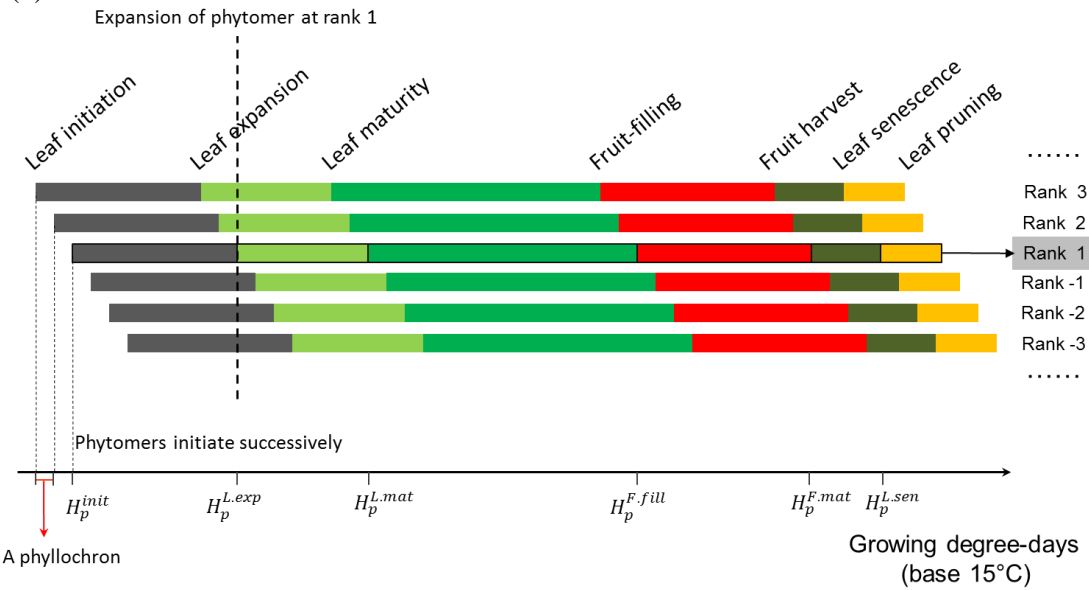
<u>Site</u>	<u>Year of planting</u>	<u>Precipitation</u> (mm yr <sup>-1</sup> )	<u>Soil type</u>	<u>Fertilization</u> (kg N ha <sup>-1</sup> yr <sup>-1</sup> )		<u>Comments</u>
				<u>amount</u>	<u>period</u>	
<u>PTPN-VI</u>	<u>2002</u>	<u>2567</u>	<u>loam Acrisol</u>	<u>456</u>	<u>2008-2014</u>	<u>industrial plantation; others are smallholders</u>
<u>Pompa Air</u>	<u>2012</u>	<u>2567</u>	<u>loam Acrisol</u>	<u>-</u>	<u>-</u>	<u>N fertilization from 6-year old onward</u>
<u>HO1</u>	<u>1997</u>	<u>2567</u>	<u>loam Acrisol</u>	<u>96</u>	<u>2003-2014</u>	<u>regular fertilization</u>
<u>HO2</u>	<u>1999</u>	<u>2567</u>	<u>loam Acrisol</u>	<u>96</u>	<u>2005-2014</u>	<u>regular fertilization</u>
<u>HO3</u>	<u>1996</u>	<u>2567</u>	<u>loam Acrisol</u>	<u>96</u>	<u>2002-2014</u>	<u>regular fertilization</u>
<u>HO4</u>	<u>2003</u>	<u>2567</u>	<u>loam Acrisol</u>	<u>96</u>	<u>2009-2014</u>	<u>regular fertilization</u>
<u>BO2</u>	<u>2000</u>	<u>2902</u>	<u>clay Acrisol</u>	<u>24</u>	<u>2006-2012</u>	<u>reduced fertilization</u>
<u>BO3</u>	<u>2001</u>	<u>2902</u>	<u>clay Acrisol</u>	<u>24</u>	<u>2007-2012</u>	<u>reduced fertilization</u>
<u>BO4</u>	<u>2002</u>	<u>2902</u>	<u>clay Acrisol</u>	<u>24</u>	<u>2008-2012</u>	<u>reduced fertilization</u>
<u>BO5</u>	<u>2004</u>	<u>2902</u>	<u>clay Acrisol</u>	<u>24</u>	<u>2010-2012</u>	<u>reduced fertilization</u>

(a)



623

(b)



624

Fig. 1. (a) New sub-canopy phytomer structure of CLM-Palm.  $P^1$  to  $P^n$  indicate expanded phytomers and  $P^{-1}$  to  $P^{-n}$  at the top indicate unexpanded phytomers packed in the bud. Each phytomer has its own phenology, represented by different colors corresponding to: (b) the phytomer phenology: from initiation to leaf expansion, to leaf maturity, to fruit-fill, to harvest, to senescence and to pruning. Phytomers initiate successively according to the phyllochron (the period in heat unit between initiations of two subsequent phytomers). Detailed phenology description is in Supplementary materials.

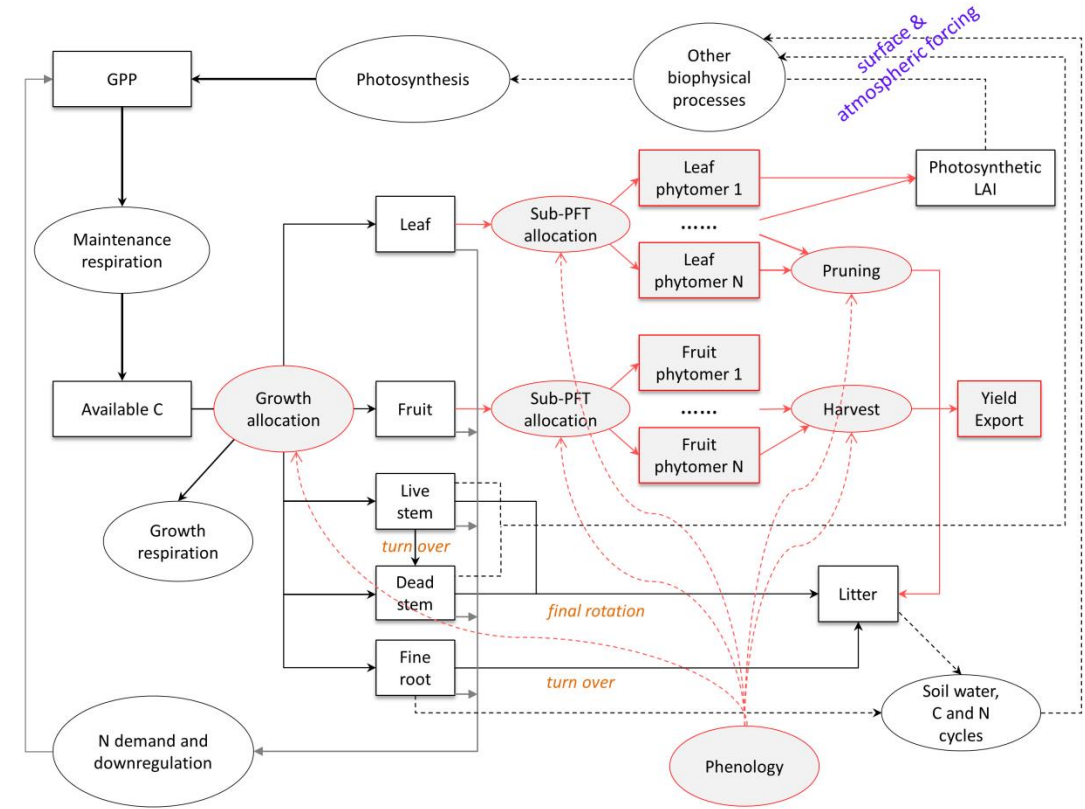
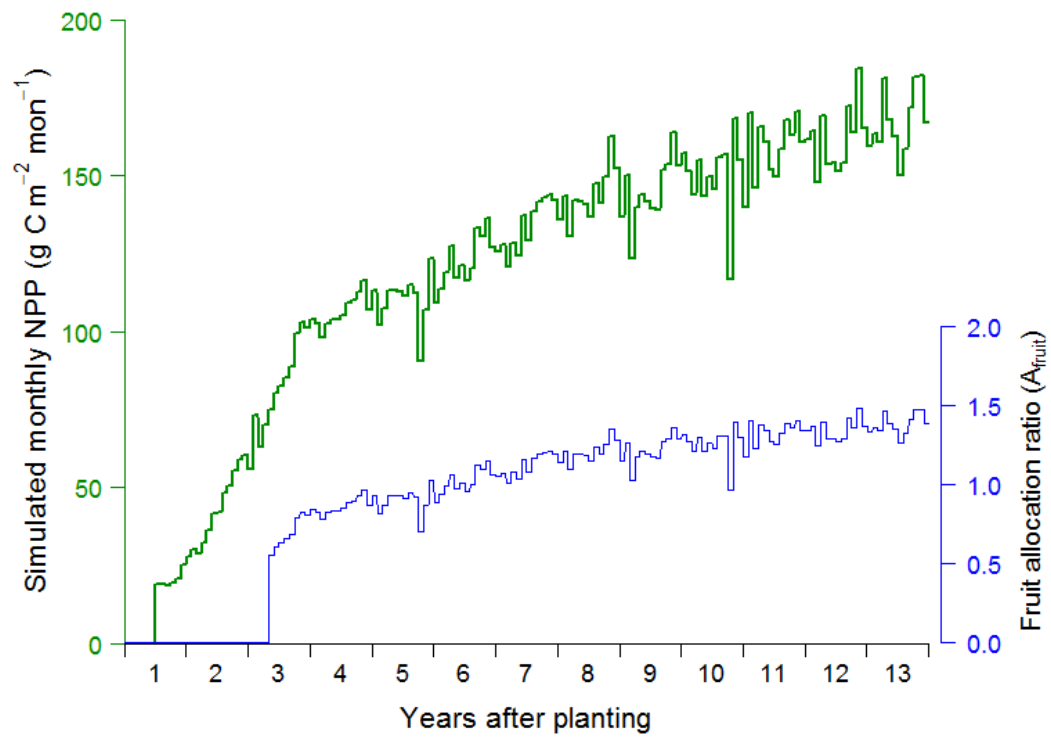


Fig. 2. Original and modified structure and functions for developing CLM-Palm in the framework of CLM4.5. Original functions from CLM4.5 are represented in black or grey. New functions designed for CLM-Palm are represented in red, including phenology, allocation, pruning, fruit harvest and export, as well as the sub-canopy (sub-PFT) structure.





639

640 Fig. 3. Time course of reproductive allocation rate (blue line) in relation to monthly NPP from  
 641 the previous month ( $NPP_{mon}$ , green line) according to Eq. 5.  $A_{fruit}$  is relative to the vegetative  
 642 unity ( $A_{leaf} + A_{stem} + A_{root} = 1$  and  $0 \leq A_{fruit} \leq 2$ ). The  $NPP_{mon}$  was simulated with  
 643 calibrated parameters for the PTPN-VI site.

644

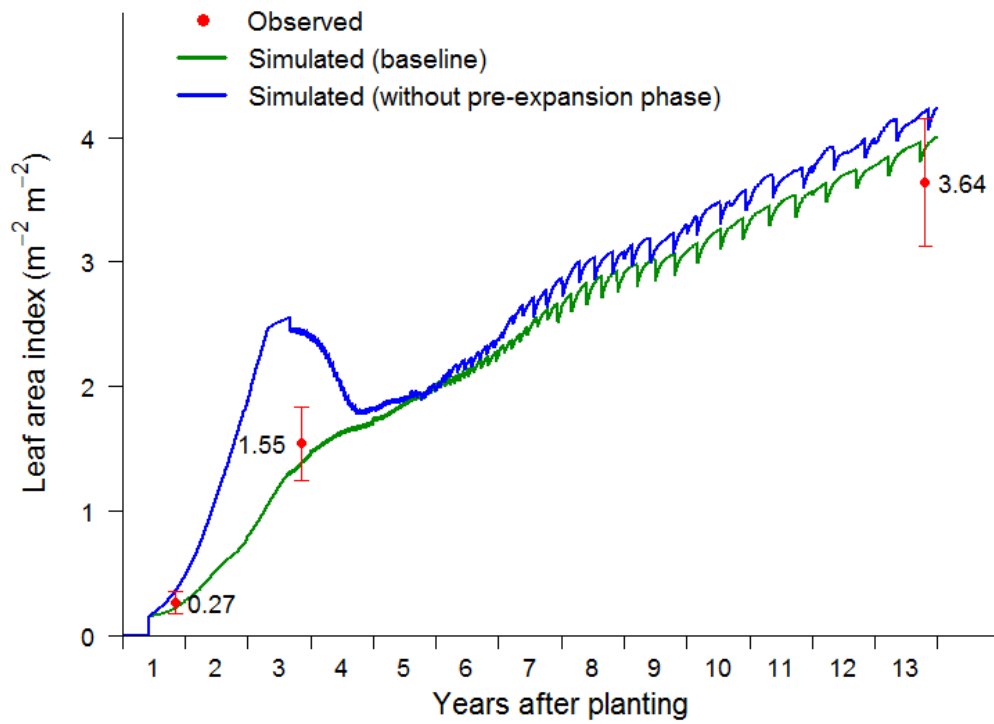
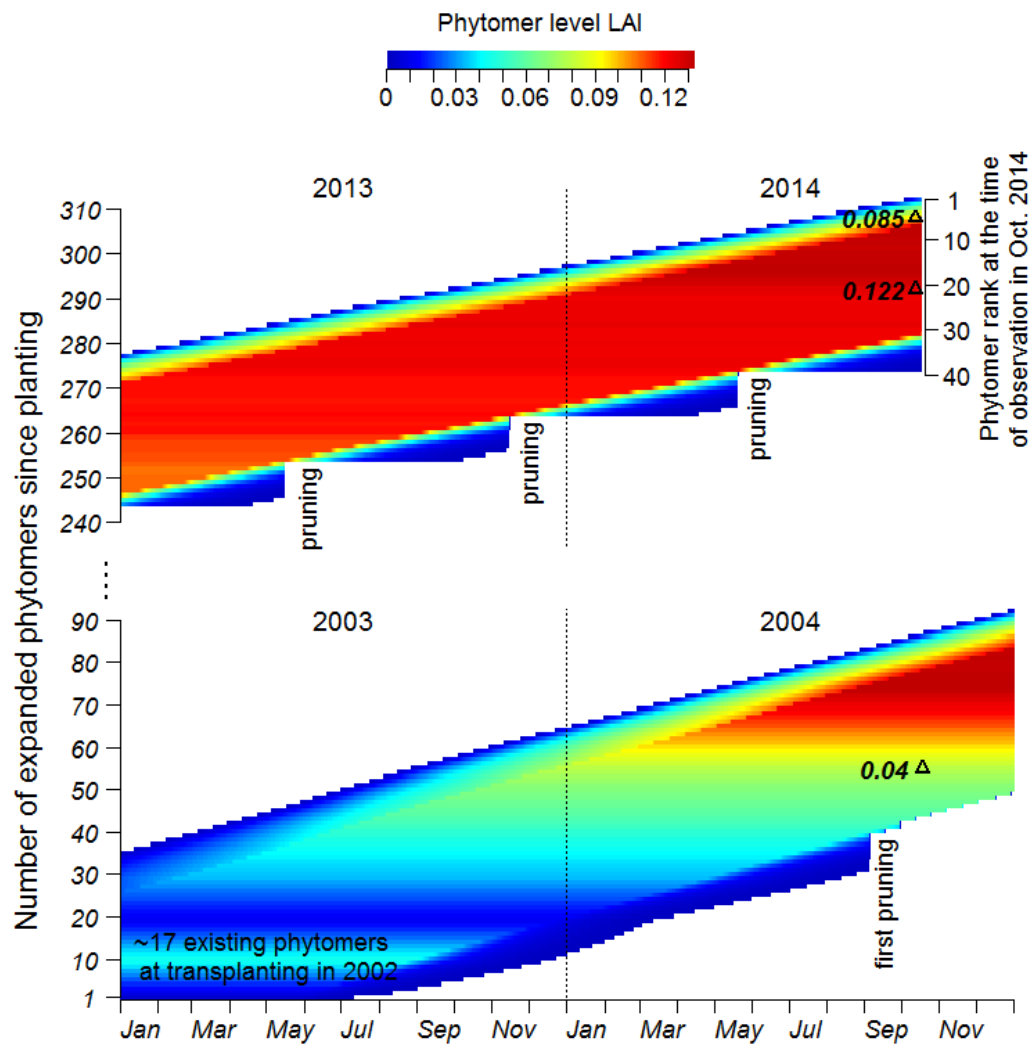


Fig. 4. PFT-level LAI simulated by CLM-Palm, with and without the pre-expansion growth phase in the phytomer phenology and compared to field measurements used for calibration. The initial sudden increase at year 1 represents transplanting from nursery. The sharp drops mark pruning events.



651

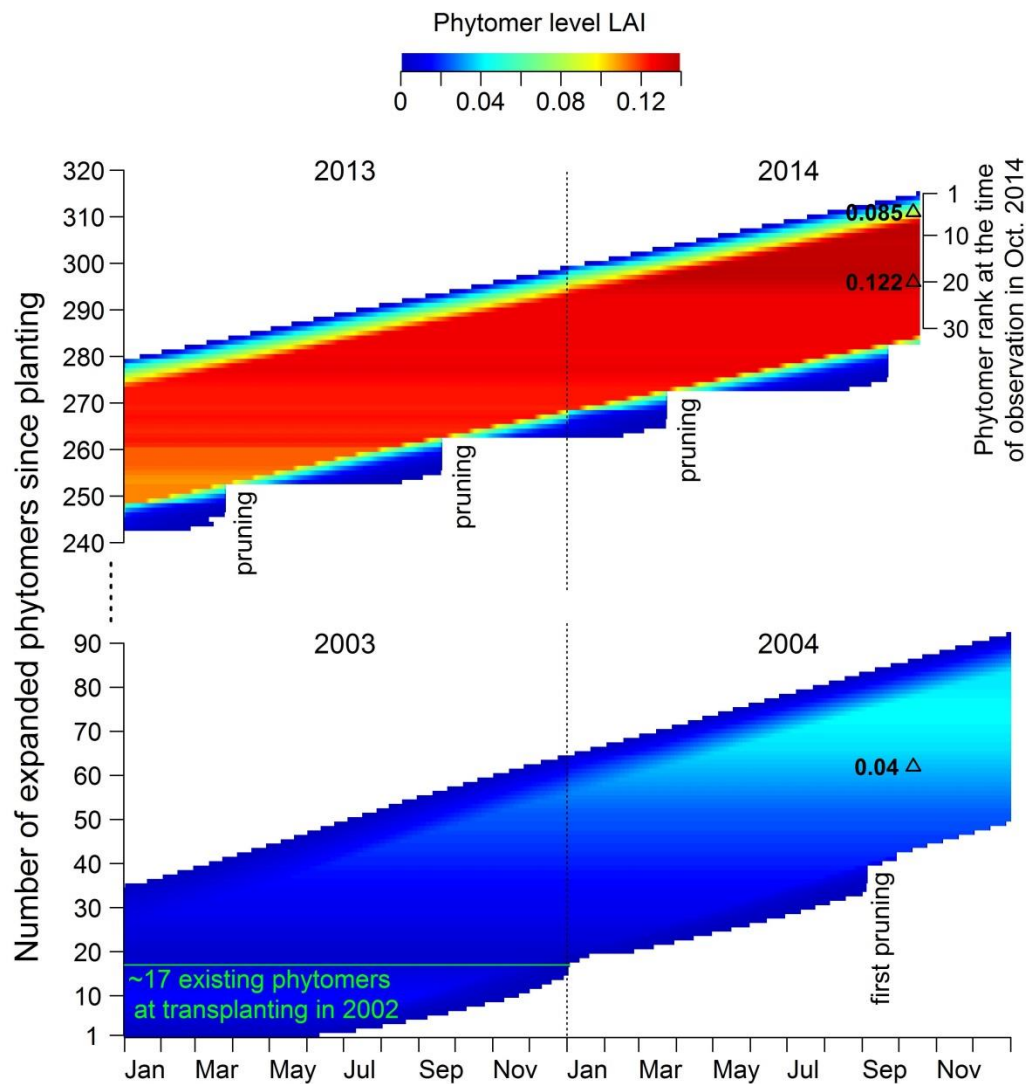


Fig. 5. Simulated phytomer level LAI dynamics (horizontal color bar) compared with field observations (black triangles with measured LAI values). A phytomer in the model is only meant to represent the average condition of an age-cohort of actual oil palm phytomers across the whole plantation landscape. The newly expanded phytomer at a given point of time has a rank of 1. Each horizontal bar represents the life cycle of a phytomer after leaf expansion. Phytomers emerge in sequence and the y-axis gives the total number of phytomers that have expanded since transplanting in the field. Senescent phytomers are pruned.

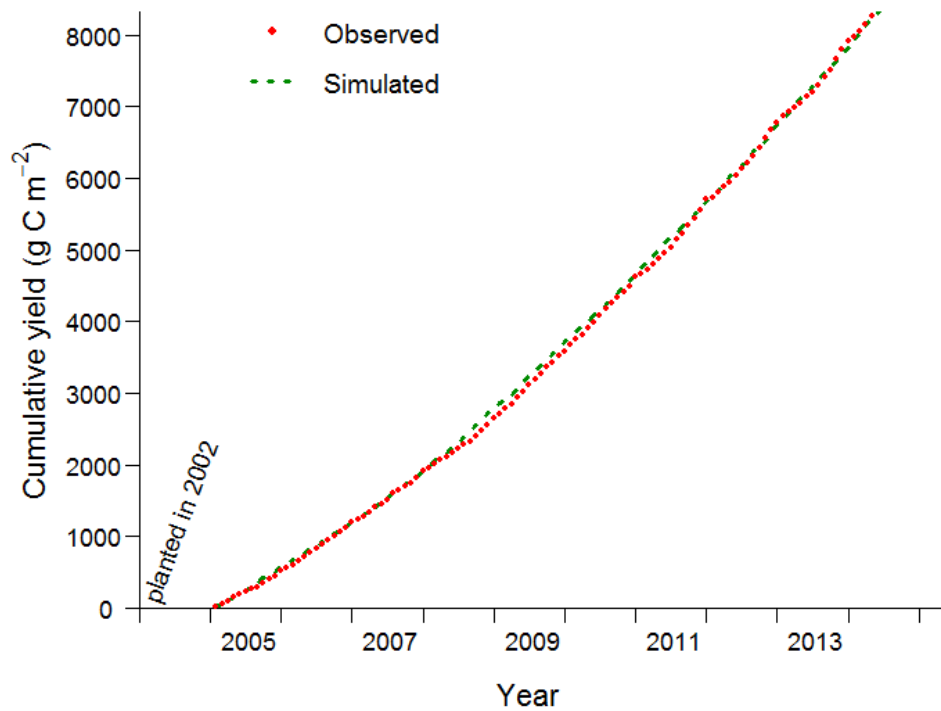


Fig. 6. Simulated PFT-level yield compared with monthly harvest data (2005-2014) from the calibration site PTPN-VI in Jambi, Sumatra. CLM-Palm represents multiple harvests from different phytomers (about twice per month). The cumulative harvest amounts throughout time are compared.

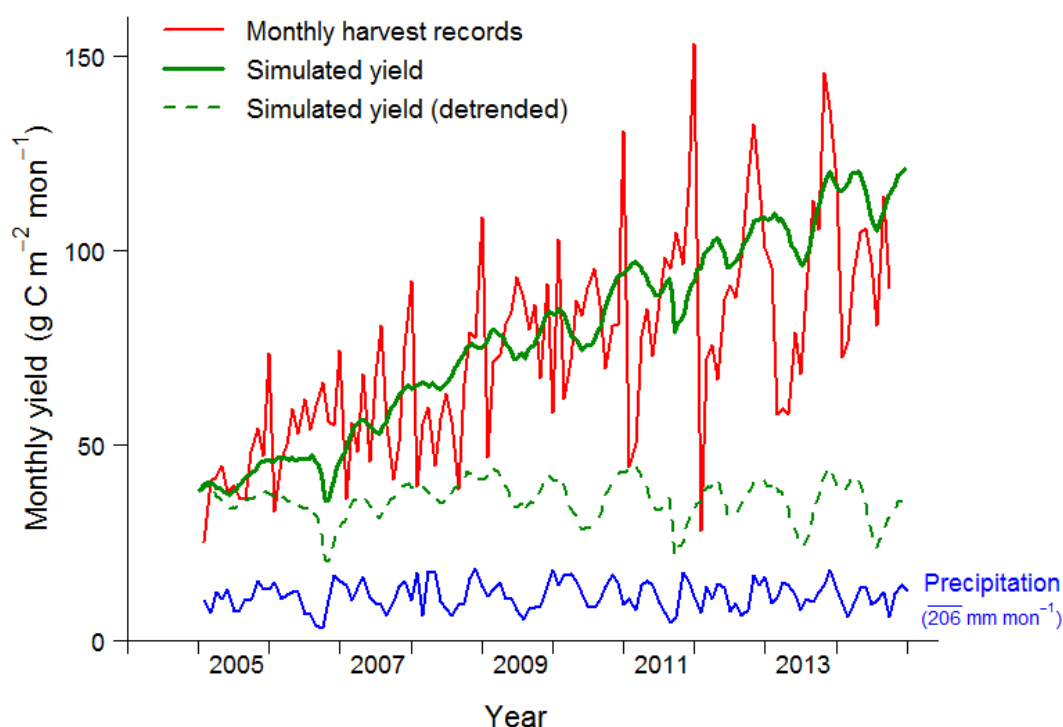
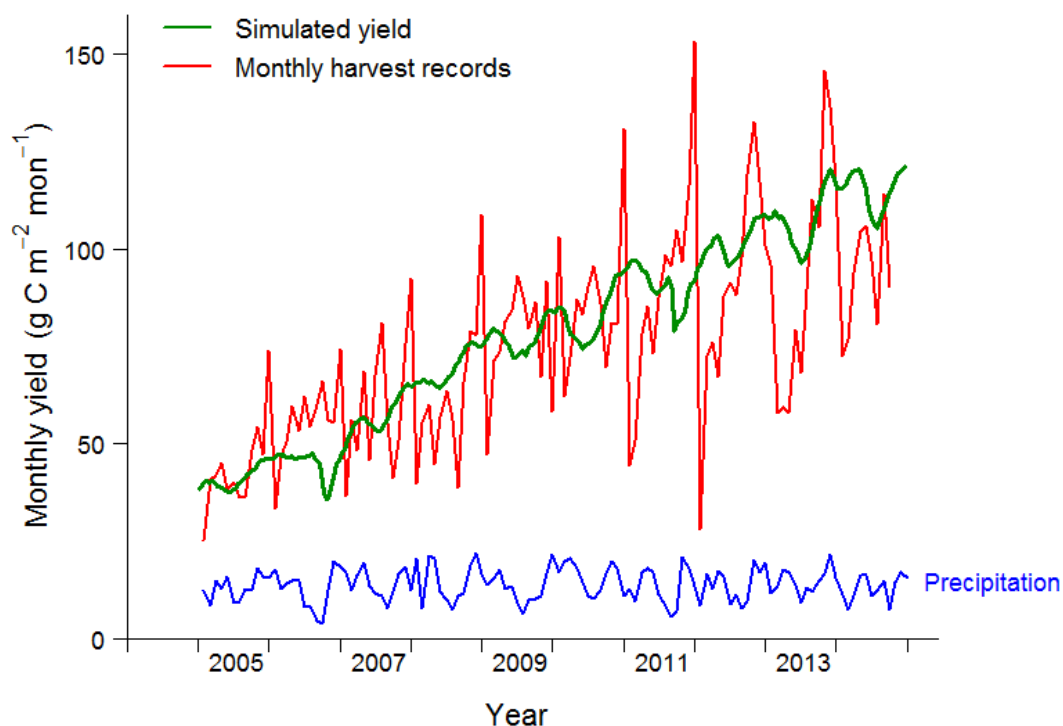


Fig. 7. Comparison of simulated and observed monthly yield at PTPN-VI compared with monthly precipitation dynamics (mean: 206 mm per month). The modeled yield outputs are per harvest event (every 15-20 days depending on the phyllochron), while harvest records are the summary of harvest events per month. The model output is thus rescaled to show the

monthly trend of yield that matches the mean of harvest records, given that the cumulative yields are almost the same between simulation and observation as shown in Fig. 6. The detrended curve is to facilitate comparison with the dynamics of monthly mean precipitation.

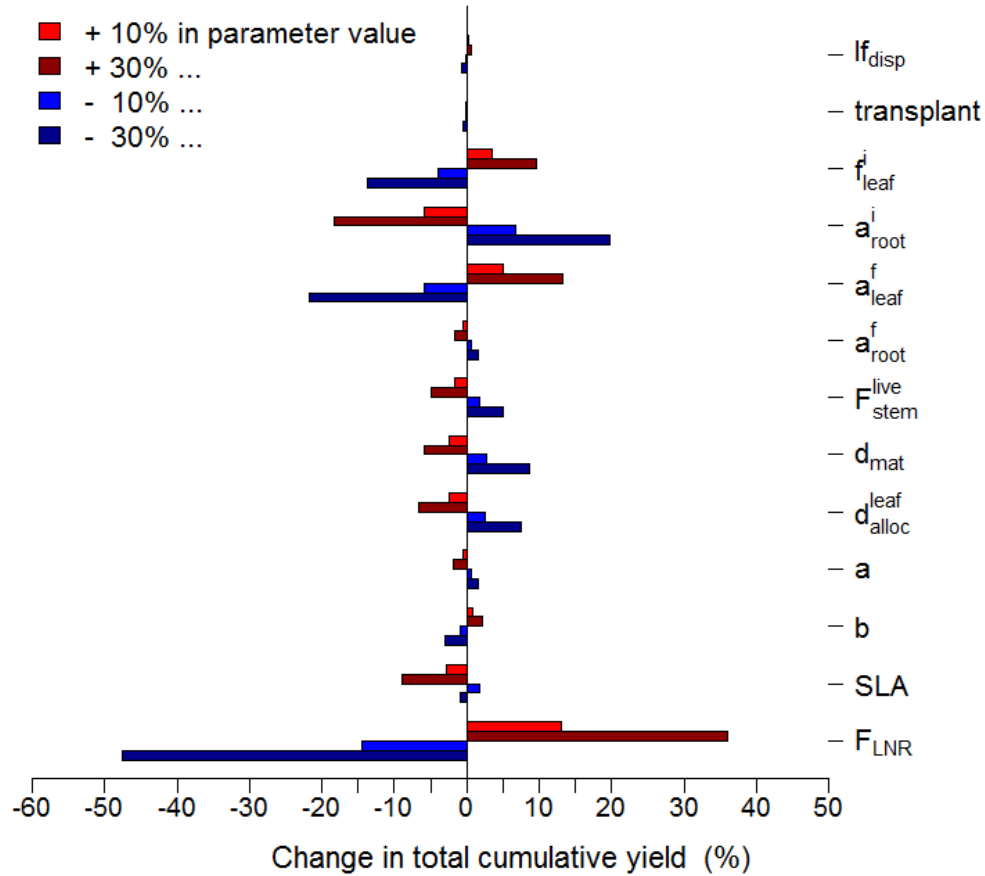


Fig. 8. Sensitivity analysis of key allocation parameters in regard of the cumulative yield at the end of simulation, with two magnitudes of change in the value of a parameter one-by-one while others are hold at the baseline values in Table A2.

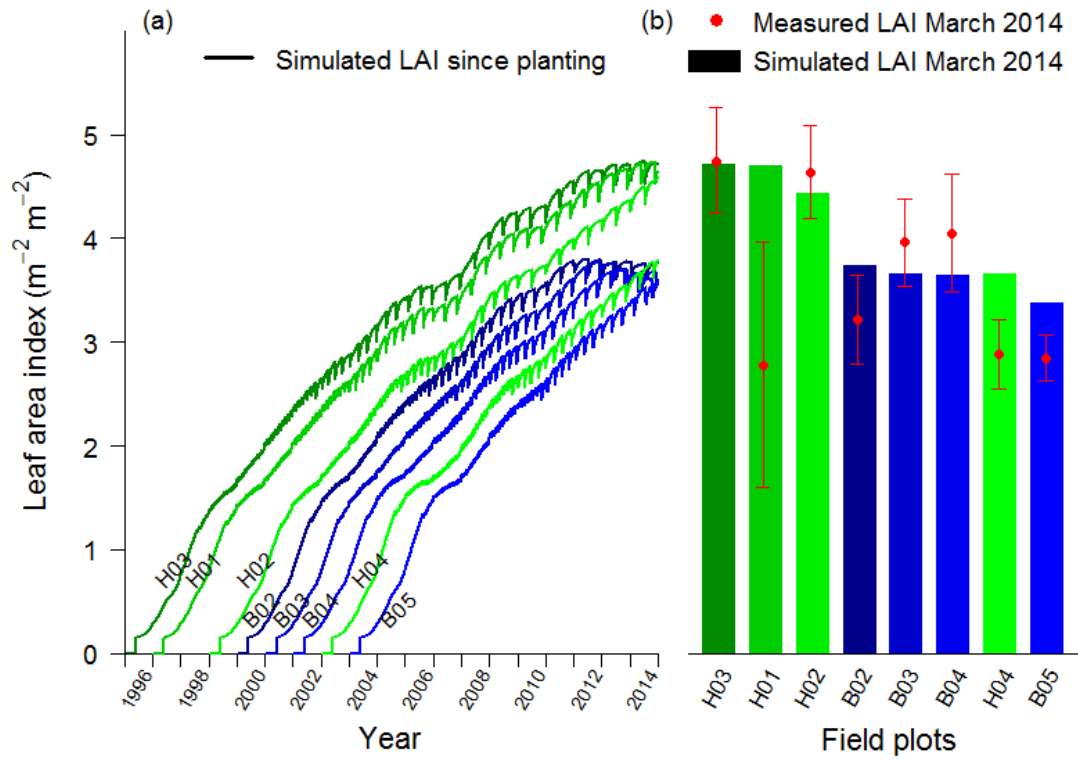
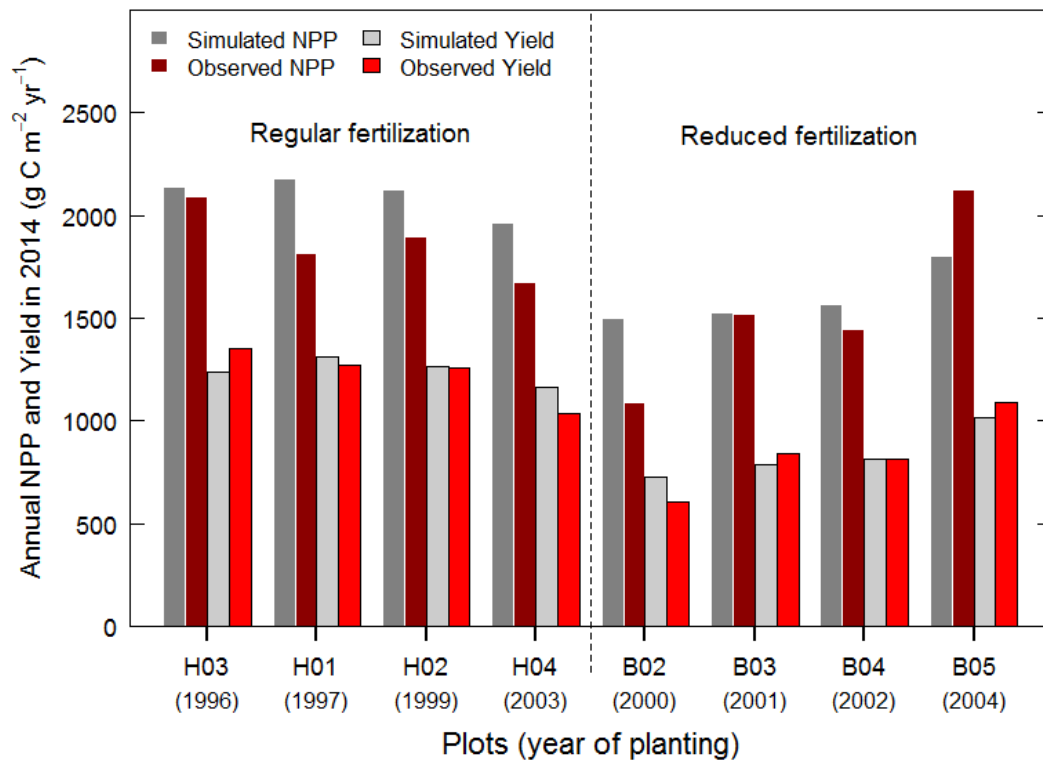


Fig. 9. Validation of LAI with 8 independent oil palm sites (sequence in plantation age) from the Harapan (regular fertilization) and Bukit Duabelas (reduced fertilization) regions: (a) shows the LAI development of each site simulated by the model since planting; (b) shows the comparison of field measured LAI in 2014 with model.





686

687 Fig. 10. Validation of yield and NPP with 8 independent oil palm sites from the Harapan (H)  
 688 and Bukit Duabelas (B) regions with different fertilization treatments. Field data were  
 689 collected in 2014.

## 690 Appendix A

### 691 Summary of main parameters

692 Table A1. Summary of new phenological parameters introduced for the phenology subroutine of CLM-Palm. The default values were determined by  
 693 calibration and with reference to field observations and literatures on oil palm (Combres et al., 2013; Corley and Tinker, 2003; Hormaza et al., 2012; Legros  
 694 et al., 2009).

Parameter	Default	Min	Max	Explanation (Unit)
$GDD_{init}$	0	0	1500	GDD needed from planting to the first phytomer initiation (°days). Initiation refers to the start of active accumulation of leaf C. A value 0 implies transplanting.
$GDD_{exp}$	1550	0	8000	GDD needed from leaf initiation to start of leaf expansion for each phytomer (pre-expansion) (°days)
$GDD_{L.mat}$	1250	500	1600	GDD needed from start of leaf expansion to leaf maturity for each phytomer (post-expansion) (°days)
$GDD_{F.fill}$	3800	3500	4200	GDD needed from start of leaf expansion to beginning of fruit-fill for each phytomer (°days)
$GDD_{F.mat}$	5200	4500	6500	GDD needed from start of leaf expansion to fruit maturity and harvest for each phytomer (°days)
$GDD_{L.sen}$	6000	5000	8000	GDD needed from start of leaf expansion to beginning of senescence for each phytomer (°days)
$GDD_{end}$	6650	5600	9000	GDD needed from start of leaf expansion to end of senescence for each phytomer (°days)
$GDD_{min}$	7500	6000	10000	GDD needed from planting to the beginning of first fruit-fill (°days)
$Age_{max}$	25	20	30	Maximum plantation age (productive period) from planting to final rotation /replanting (years)
$PLAI_{max}$	0.165	0.1	0.2	Maximum LAI of a single phytomer ( $m^2 m^{-2}$ )
$mxlivenp$	40	30	50	Maximum number of expanded phytomers coexisting on a palm
$phyllochron$	130	100	160	Initial phyllochron (=plastochron): the period in heat unit between the initiations of two successive phytomers. The value increases to 1.5 times, i.e. 195, at 10-year old (°days)

695 Table A2. Summary of parameters involved in C and N allocation. The default values were determined by calibration and with reference to field  
696 measurements (Kotowska et al., 2015a).

Parameter	Defaults	Min	Max	Explanation (Unit)
$*l_{disp}^i$	0.3	0.1	1	Fraction of C and N allocated to the displayed leaf pool
$*transplant$	0.15	0	0.3	Initial total LAI assigned to existing expanded phytomers at transplanting. Value 0 implies planting as seeds.
$f_{leaf}^i$	0.15	0	1	Initial value of leaf allocation coefficient before the first fruit-fill
$a_{root}^i$	0.3	0	1	Initial value of root allocation coefficient before the first fruit-fill
$a_{leaf}^f$	0.28	0	1	Final value of leaf allocation coefficient after vegetative maturity
$a_{root}^f$	0.1	0	1	Final value of root allocation coefficient after vegetative maturity
$F_{stem}^{live}$	0.15	0	1	Fraction of new stem allocation that goes to live stem tissues, the rest to metabolically inactive stem tissues
$d_{mat}$	0.6	0.1	1	Factor to control the age when the leaf allocation ratio stabilizes at $a_{leaf}^f$ according to Eq. 4
$d_{alloc}^{leaf}$	0.6	0	5	Factor to control the nonlinear function in Eq. 4. Values < 1 give a convex curve and those > 1 give a concave curve. Value 1 gives a linear function.
$*a$	0.2	0	1	Parameter $a$ for fruit allocation coefficient $A_{fruit}$ in Eq. 5
$*b$	0.02	0	1	Parameter $b$ for fruit allocation coefficient $A_{fruit}$ in Eq. 5
$SLA$	0.013	0.01	0.015	Specific leaf area ( $m^2 g^{-1} C$ )
$F_{LNR}$	0.1005	0.05	0.1	Fraction of leaf <del>nitrogen</del> N in Rubisco enzyme. Used together with $SLA$ to calculate $V_{cmax25}$ ( $g N Rubisco g^{-1} N$ )

697 \*New parameters introduced for oil palm. Others are existing parameters in CLM but mostly are redefined or used in changed context.

698 Table A3. Other optical, morphological, and physiological parameters for oil palm.

Parameter	Value	Definition (Unit)	Comments
$CN_{leaf}$	33	Leaf <del>carbon-to-nitrogen</del> C:N ratio (g C g <sup>-1</sup> N)	By leaf C:N analysis
$CN_{root}$	42	Root <del>C:N</del> carbon-to-nitrogen ratio (g C g <sup>-1</sup> N)	Same as all other PFTs
$CN_{livewd}$	50	Live stem <del>C:N</del> carbon-to-nitrogen ratio (g C g <sup>-1</sup> N)	Same as all other PFTs
$CN_{deadwd}$	500	Dead stem <del>C:N</del> carbon-to-nitrogen ratio (g C g <sup>-1</sup> N)	Same as all other PFTs
$CN_{flit}$	60	Leaf litter <del>C:N</del> carbon-to-nitrogen ratio (g C g <sup>-1</sup> N)	Same as other tree PFTs
$CN_{fruit}$	75	Fruit <del>C:N</del> carbon-to-nitrogen ratio (g C g <sup>-1</sup> N)	Higher than the value 50 for other crops because of high oil content in palm fruit
$r_{vis/nir}^{leaf}$	0.09/0.45	Leaf reflectance in the visible (VIS) or near-infrared (NIR) bands	Values adjusted in-between trees and crops
$r_{vis/nir}^{stem}$	0.16/ 0.39	Stem reflectance in the visible or near-infrared bands	Values adjusted in-between trees and crops
$\tau_{vis/nir}^{leaf}$	0.05/0.25	Leaf transmittance in the visible or near-infrared bands	Values adjusted in-between trees and crops
$\tau_{vis/nir}^{stem}$	0.001/ 0.001	Stem transmittance in the visible or near-infrared bands	Values adjusted in-between trees and crops
$\chi_L$	-0.4	Leaf angle distribution index for radiative transfer (0 = random leaves; 1 = horizontal leaves; -1 = vertical leaves)	Estimated by field observation. In CLM, $-0.4 \leq \chi_L \leq 0.6$
$taper$	50	Ratio of stem height to radius-at-breast-height	Field observation. Used together with <i>stocking</i> and <i>dwood</i> to calculate canopy top and bottom heights.
<i>stocking</i>	150	Number of palms per hectare (stems ha <sup>-2</sup> )	Field observation. Used to calculate stem area index (SAI) by: $SAI = 0.05 \times LAI \times stocking$ .

$d_{wood}$	100000	Wood density ( $\text{gC m}^{-3}$ )	Similar as coconut palm (O. Roupsard, personal communication)
$R_{z0m}$	0.05	Ratio of momentum roughness length to canopy top height	T. June, personal communication
$R_d$	0.76	Ratio of displacement height to canopy top height	T. June, personal communication

---

- Allen, K., Corre, M. D., Tjoa, A., and Veldkamp, E.: Soil nitrogen-cycling responses to conversion of lowland forests to oil palm and rubber plantations in Sumatra, Indonesia, *PLoS ONE*, 10(7), e0133325, doi:10.1371/journal.pone.0133325, 2015
- Bonan, G. B., Levis, S., Kergoat, L., and Oleson, K. W.: Landscapes as patches of plant functional types: An integrated concept for climate and ecosystem models, *Global Biogeochemical Cycles*, 16 (2), 1021-1051, 2002.
- Carlson, K. M., Curran, L. M., Asner, G. P., Pittman, A. M., Trigg, S. N., and Adeney, J. M.: Carbon emissions from forest conversion by Kalimantan oil palm plantations, *Nature Clim. Change*, 3(3), 283–287, doi:10.1038/nclimate1702, 2012.
- Carrasco, L. R., Larrosa, C., Milner-Gulland, E. J., and Edwards, D. P.: A double-edged sword for tropical forests, *Science*, 346(6205), 38-40, 2014.
- Combres, J.-C., Pallas, B., Rouan, L., Mialet-Serra, I., Caliman, J.-P., Braconnier, S., Soulie, J.-C., and Dingkuhn, M.: Simulation of inflorescence dynamics in oil palm and estimation of environment-sensitive phenological phases: a model based analysis, *Functional Plant Biology*, 40(3), 263-279, 2013.
- Corley R. H. V. and Tinker, P. B. (Eds.): *The oil palm*, 4th edition, Blackwell Science, Oxford, 2003.
- Dee, D. P., Uppala, S. M., Simmons, A. J., Berrisford, P., Poli, P., Kobayashi, S., ... and Vitart, F.: The ERA-Interim reanalysis: Configuration and performance of the data assimilation system, *Quarterly Journal of the Royal Meteorological Society*, 137(656), 553-597, 2011.
- Drewniak, B., Song, J., Prell, J., Kotamarthi, V. R., and Jacob, R.: Modeling agriculture in the community land model, *Geoscientific Model Development*, 6(2), 495-515, doi:10.5194/gmd-6-495-2013, 2013.
- Euler, M.: *Oil palm expansion among Indonesian smallholders - adoption, welfare implications and agronomic challenges*, Ph.D. thesis, University of Göttingen, Germany, 145 pp., 2015.
- FAO. FAOSTAT Database, Food and Agriculture Organization of the United Nations, Rome, Italy, available at: <http://faostat.fao.org/site/339/default.aspx> (last access: ~~17 June~~ 31 October 2015), 2013.
- Galloway, J. N., Dentener, F. J., Capone, D. G., Boyer, E. W., Howarth, R. W., Seitzinger, S. P., ... and Vösmarty, C. J.: Nitrogen cycles: past, present, and future, *Biogeochemistry*, 70(2), 153-226, 2004.
- Georgescu, M., Lobell, D. B., and Field, C. B.: Direct climate effects of perennial bioenergy crops in the United States, *Proceedings of the National Academy of Sciences*, 108(11), 4307-4312, 2011.
- Goh K. J.: Climatic requirements of the oil palm for high yields, in: *Managing oil palm for high yields: agronomic principles*, Goh K.J. (Eds.), pp. 1–17, Malaysian Soc. Soil Sci. and Param Agric. Surveys, Kuala Lumpur, 2000.
- Guillaume, T., Damris, M., and Kuzyakov, Y.: Losses of soil carbon by converting tropical forest to plantations: erosion and decomposition estimated by  $\delta^{13}\text{C}$ , *Global change biology*, 21, 3548–3560, doi: 10.1111/gcb.12907, 2015.
- Gunarso, P., Hartoyo, M. E., Agus, F., and Killeen, T. J.: Oil Palm and Land Use Change in Indonesia, Malaysia, and Papua New Guinea. In: Killeen T, Goon J, editors. *Reports from the Science Panel of the Second GHG Working Group of the Roundtable for Sustainable Palm Oil (RSPO)*. Kuala Lumpur, 2013.
- Hall é F., Oldeman, R. A. A. and Tomlinson, P. B.: *Tropical trees and forests. An architectural analysis*. Springer-Verlag, Berlin, 441 pp., 1978.
- Hijmans, R. J., Cameron, S. E., Parra, J. L., Jones, P. G., and Jarvis, A.: Very high resolution interpolated climate surfaces for global land areas, *International journal of climatology*, 25(15), 1965-1978, 2005.

- Hoffmann, M. P., Vera, A. C., Van Wijk, M. T., Giller, K. E., Oberthur, T., Donough, C., and Whitbread, A. M.: Simulating potential growth and yield of oil palm (*Elaeis guineensis*) with PALMSIM: Model description, evaluation and application, *Agricultural Systems*, 131, 1-10, 2014.
- Hormaza, P., Fuquen, E. M., and Romero, H. M.: Phenology of the oil palm interspecific hybrid *Elaeis oleifera* × *Elaeis guineensis*, *Scientia Agricola*, 69(4), 275-280, 2012.
- Huth, N. I., Banabas, M., Nelson, P. N., and Webb, M.: Development of an oil palm cropping systems model: lessons learned and future directions, *Environ. Modell. Softw.*, 62, 411–419, doi:10.1016/j.envsoft.2014.06.021, 2014.
- Jin, J. M. and Miller, N. L.: Regional simulations to quantify land use change and irrigation impacts on hydroclimate in the California Central Valley, *Theoretical and Applied Climatology*, 104, 429-442, 2011.
- Koh, L. P. and Ghazoul, J.: Spatially explicit scenario analysis for reconciling agricultural expansion, forest protection, and carbon conservation in Indonesia, *P. Natl. Acad. Sci. USA*, 107, 11140–11144, doi: 10.1073/pnas.1000530107, 2010.
- Kotowska, M. M., Leuschner, C., Triadiati T., Selis M., and Hertel, D.: Quantifying above- and belowground biomass carbon loss with forest conversion in tropical lowlands of Sumatra (Indonesia), *Global Change Biol.*, 21, 3620-3634, doi: 10.1111/gcb.12979, 2015a.
- Kotowska, M. M., Leuschner, C., Triadiati, T., and Hertel, D.: Conversion of tropical lowland forest lowers nutrient return with litterfall, and alters nutrient use efficiency and seasonality of net primary productivity, *Oecologia*, submitted, 2015b.
- Koven, C. D., Riley, W. J., Subin, Z. M., Tang, J. Y., Torn, M. S., Collins, W. D., Bonan, G. B., Lawrence, D. M., and Swenson, S. C.: The effect of vertically resolved soil biogeochemistry and alternate soil C and N models on C dynamics of CLM4, *Biogeosciences*, 10(11), 7109-7131, doi:10.5194/bg-10-7109-2013, 2013.
- Legros, S., Mialet-Serra, I., Caliman, J. P., Siregar, F. A., Clement-Vidal A., and Dingkuhn, M.: Phenology and growth adjustments of oil palm (*Elaeis guineensis*) to photoperiod and climate variability, *Annals of Botany* 104, 1171–1182. doi:10.1093/aob/mcp214, 2009.
- Levis, S., Bonan, G., Kluzek, E., Thornton, P., Jones, A., Sacks, W., and Kucharik, C.: Interactive crop management in the Community Earth System Model (CESM1): Seasonal influences on land-atmosphere fluxes, *J. Climate*, 25, 4839-4859, DOI:10.1175/JCLI-D-11-00446.1., 2012.
- Luyssaert, S., Schulze, E. D., Börner, A., Knohl, A., Hessenmüller, D., Law, B. E., Ciais, P., and Grace, J.: Old-growth forests as global carbon sinks, *Nature*, 455(7210), 213-215, 2008.
- Miettinen, J., Shi, C. H. and Liew, S. C.: Deforestation rates in insular Southeast Asia between 2000 and 2010, *Global Change Biology*, 17, 2261-2270, 2011.
- Navarro, M. N. V., Jourdan, C., Sileye, T., Braconnier, S., Mialet-Serra, I., Saint-Andre, L., ... and Rouspard, O.: Fruit development, not GPP, drives seasonal variation in NPP in a tropical palm plantation, *Tree physiology*, 28(11), 1661-1674, 2008.
- Oleson, K. W., Bonan, G. B., Levis, S., and Vertenstein, M.: Effects of land use change on North American climate: impact of surface datasets and model biogeophysics, *Climate Dynamics*, 23, 117-132, 2004.
- Oleson, K., Lawrence, D., Bonan, G., Drewniak, B., Huang, M., Koven, C., Levis, S., Li, F., Riley, W., Subin, Z., Swenson, S., Thornton, P., Bozbiyik, A., Fisher, R., Heald, C., Kluzek, E., Lamarque, J.-F., Lawrence, P., Leung, L., Lipscomb, W., Muszala, S., Ricciuto, D., Sacks, W., Sun, Y., Tang, J., and Yang, Z.-L.: Technical description of version 4.5 of the Community Land Model (CLM), National Center for Atmospheric Research, Boulder, Colorado, USA, 420 pp., doi:10.5065/D6RR1W7M, 2013.
- Tang, J. Y., Riley, W. J., Koven, C. D., and Subin, Z. M.: CLM4-BeTR, a generic biogeochemical transport and reaction module for CLM4: model development, evaluation, and application, *Geosci. Model Dev.*, 6, 127-140. doi:10.5194/gmd-6-127-2013, 2013.

806 van Kraalingen, D. W. G., Breure, C. J., and Spitters, C. J. T.: Simulation of oil palm growth  
 807 and yield, *Agricultural and forest meteorology*, 46(3), 227-244, 1989.  
 808 Veldkamp, E., and Keller, M.: Nitrogen oxide emissions from a banana plantation in the  
 809 humid tropics, *Journal of Geophysical Research: Atmospheres* (1984–2012), 102(D13),  
 810 15889-15898, 1997.  
 811 White, M. A., Thornton, P. E., and Running, S. W.: A continental phenology model for  
 812 monitoring vegetation responses to interannual climatic variability, *Global Biogeochem.*  
 813 *Cycles*, 11, 217-234, 1997.  
 814



## Supplementary materials

### Description of the oil palm phenology in CLM-Palm

The following sections describe the life cycle of each phytomer as well as the planting, stem and root turnover, and rotation (replanting) for the whole plant. Nitrogen retranslocation is implemented for each phytomer during its senescence. Summary of new phenological parameters introduced for the palm PFT is in Table A1 in the Appendix.

#### 1. Planting and leaf initiation

Planting is implemented in the similar way as in the CLM4.5 crop phenology except that  $GDD_{15}$  (growing degree-days with 15 °C base temperature) is tracked since planting and an option of transplanting is enabled. An initial phytomer emergence threshold ( $GDD_{init}$ ) is prescribed for attaining the first leaf initiation after planting (Table A1). When  $GDD_{init}$  is zero, it implies transplanting from nursery instead of seed sowing in the field. Oil palm seedlings usually grow in nursery for 1-2 year before being transplanted into the field. Therefore, in this study  $GDD_{init}$  is set to zero and the first new phytomer is assumed to initiate immediately after transplanting in the field. An initial total leaf area index (LAI) of 0.15 is assigned to the existing expanded phytomers, whose leaf sizes are restricted to be within 10% of the maximum phytomer LAI ( $PLAI_{max}$ ) (Table A2).

The oil palm phytomers initiate as leaf primordia in the apical bud and then appear as leaves on the stem successively according to relatively stable intervening periods, termed plastochron (the duration in terms of heat unit (GDD) between successive leaf initiation events) and phyllochron (the rate of leaf emergence from the apical bud). Here for simplicity, the phyllochron is assumed equal to the plastochron. As the apical buds in palms usually do not start to accumulate dry mass immediately after physiological initiation but wait until several phyllochrons before expansion (Navarro et al., 2008), we define leaf initiation as the

start of active accumulation of leaf C in this model, so that the phenological steps and C and N allocation process can be at the same pace.

A parameter *phyllochron* is prescribed with an initial value of 130 degree-days at planting with reference to  $GDD_{15}$  and it increases linearly to 1.5 times at 10-year old (Huth et al., 2014). Given  $GDD_{init}$  and *phyllochron*, a heat unit index  $H_p^{init}$  for triggering leaf initiation can be calculated for each new phytomer when a preceding phytomer initiates:

$$\begin{aligned} H_1^{init} &= GDD_{init} \\ H_{p+1}^{init} &= H_p^{init} + \textit{phyllochron} \end{aligned} \quad \text{Eq. S1}$$

where subscripts  $p$  and  $p+1$  refer to successive phytomers and  $1$  refers to the first new phytomer initiated after planting.

As the GDD accumulates since planting, new phytomers will be turned on in sequence when  $GDD_{15} > H_p^{init}$ , and will enter the 7-step life cycle one by one. The timing of later phenological steps for each new phytomer is determined at the time of initiation by adding the length of a corresponding phase period (Table A1). Each newly initiated phytomer is assigned a negative rank of  $-N$  and remains packed in the bud until the next phase of leaf expansion is triggered. The oldest unexpanded phytomer (spear leaf), right before expansion, has a rank of  $-1$ . The GDD period between leaf initiation and expansion is used to calculate the number of bud phytomers that have already initiated before transplanting, i.e.  $N = \frac{GDD_{exp}}{\textit{phyllochron}}$ .

## 2. Leaf expansion

During the phase from initiation to leaf expansion, leaf C already starts to build-up in the bud or spear leaf but it remains photosynthetically inactive. The thermal threshold for leaf expansion is calculated by  $H_p^{exp} = H_p^{init} + GDD_{exp}$ . Only when  $GDD_{15} > H_p^{exp}$  for a phytomer ranked  $-1$ , the leaf starts to expand and becomes photosynthetically active. Its rank

changes to a positive value of 1, while the ranks of other phytomers all increase by 1 at the same time. The expansion phase lasts for roughly 5-6 phyllochrons until leaf maturity (Legros et al., 2009).

Hereafter, the pre-expansion and post-expansion growth periods, distinguished by negative and positive ranks, are treated separately so as to differentiate non-photosynthetic and photosynthetic increases in leaf C. The following post-expansion phases and their thresholds are determined with reference to  $H_p^{exp}$ .

### 3. Leaf maturity

Another phenological step is added for the timing of leaf maturing so as to control the period of post-expansion leaf growth for each phytomer. An oil palm leaf usually reaches maturity well before fruit-fill starts on the same phytomer. Therefore, we set the parameter  $GDD_{L.mat}$  to be smaller than  $GDD_{F.fill}$  (Table A1) so that post-expansion leaf growth continues for 2-3 months (5-6 phyllochrons) and stops around 6 months before fruit-fill. The phenological threshold  $H_p^{L.mat}$  is calculated as  $H_p^{L.mat} = H_p^{exp} + GDD_{L.mat}$ .

### 4. Fruit filling

Fruit-fill starts on a phytomer when  $GDD_{15}$  exceeds a heat unit index  $H_p^{F.fill}$ . This threshold is calculated by  $H_p^{F.fill} = H_p^{exp} + GDD_{F.fill}$ . At this point, the phytomer enters reproductive growth. Growth allocation increases gradually for the fruit component while leaf C and LAI remain constant on the mature phytomer until senescence. Due to the fact that most inflorescences on the initial phytomers within 2 years after planting are male (Corley and Tinker, 2003), another threshold  $GDD_{min}$  is used to control the beginning of first fruiting on the palm. Only when  $GDD_{15} > GDD_{min}$ , the mature phytomers are allowed to start fruit-filling.

## 5. Fruit harvest and output

Fruit harvest occurs at one time step when a phytomer reaches fruit maturity, measured by a heat unit index  $H_p^{F.mat} = H_p^{exp} + GDD_{F.mat}$ . Since GDD build-up is weather dependent and phyllochron increases through aging, the harvest interval is not constant. New variables track the flow of fruit C and N harvested from each phytomer to PFT-level crop yield output pools. The fruit C and N outputs are isolated and are not involved in any further processes such as respiration and decomposition, although their fate is largely uncertain.

## 6. Litter fall

For oil palm, leaf litter-fall is performed in two phases: senescence and pruning. Senescence is simulated as a gradual reduction in photosynthetic leaf C and N on the bottom phytomers when  $GDD_{15} > H_p^{L.sen}$ , where  $H_p^{L.sen} = H_p^{exp} + GDD_{L.sen}$ . These phytomers are allowed to stay on the palm until pruning is triggered. Their senescence rates are calculated as the inverse of the remaining time until the end of a phytomer's life cycle ( $GDD_{end}$ ). Leaf C removed during this phase is not put into the litter pool immediately but saved in a temporary pool  $C_{leaf}^{senescent}$  until pruning, while the photosynthetic LAI of senescent phytomers are updated at every time step. The reason to do this is that each oil palm frond is a big leaf attached tightly to the stem and its leaflets do not fall to the ground during senescence unless the whole frond is pruned. Thus, the dynamics of soil litter pool and decomposition process could be represented better with this function. Nitrogen from senescent phytomers is remobilized to a separate N retranslocation pool that contributes to photosynthetic N demand of other phytomers and avoids supplying excessive amount of N to the litter. The proportion of N remobilized from senescent leaves before pruning is adjusted by the length of senescent period ( $GDD_{end} - GDD_{L.sen}$ ) with a given pruning frequency, and the rest N goes to the litter pool.

Pruning is conducted at one time step if the number of expanded phytomers (including senescent ones) exceeds the maximum number allowed on a palm ( $mxlivenp$ ). All senescent phytomers are subject to pruning at the time of harvest and their remaining C and N together with the temporary  $C_{leaf}^{senescent}$  pool are moved to the litter pool immediately. The frequency and intensity of pruning is determined through the combination of  $mxlivenp$ ,  $GDD_{L, sen}$  and  $phyllochron$ . A larger  $mxlivenp$  gives lower pruning frequency and a smaller  $GDD_{L, sen}$  results in more senescent leaves being pruned at one time. Besides, since  $phyllochron$  increases by age, the rate of phytomer emergence decreases and thus pruning frequency also decreases when the plantation becomes older.

## 7. Stem, roots and rotation

Unlike other crops, the oil palm stem is represented by two separate pools for live and dead stem tissues (Fig. 1a). Although the stem of oil palm is not truly woody, field observations have found that the stem section below the lowest phytomer only contains less than 6% of live tissues in the core of trunk for transporting assimilates to the roots (van Kraalingen et al., 1989). This is similar to the stem of most woody trees that largely consists of functionally dead lignified xylem. Therefore, conversion from live to dead stem for oil palm follows the CLM stem turnover function for trees, except that the turnover rate is slightly adjusted to be the inverse of leaf longevity (in seconds), such that when a leaf is dead the stem section below it will mostly become dead. Leaf longevity is around 1.6 years measured from leaf expansion to the end of senescence. The oil palm fine-root turnover follows the CLM scheme for trees and crops which also uses a turnover rate as the inverse of leaf longevity. When the maximum plantation age (usually 25 years) of oil palm is reached and a new rotation cycle starts, the whole PFT is turned off and all C and N of the leaves, stem and roots go to litter. Existing fruit C and N of mature phytomers go to the fruit output pools. The PFT is then replanted in the next year and enters new phenological cycles.